https://doi.org/10.5194/essd-2026-198
Preprint. Discussion started: 8 April 2026

Open Access Earth System Science Data Discussions

The Greenland GNSS Network (GNET): Geodetic Grade GNSS measurements of Greenland's 3D Bedrock Displacement from 1995 - 2025

Christian Solgaard[1], Finn Bo Madsen[1], Malte Winther-Dahl[2], Thomas Henry Nylen[1], Danjal Longfors Berg[1], Ole Bjerregaard[1], Javed Hassan[1], Per Knudsen[1], Michael Bevis[3], and Shfaqat Abbas Khan[1]

[1]DTU Space - National Space Institute, Technical University of Denmark, Department of Geodesy and Earth Observation, 2800 Kgs. Lyngby, Denmark
[2]Agency for Climate Data, 2100 København Ø, Denmark
[3]School of Earth Sciences, Ohio State University, Columbus, Ohio, USA

Correspondence: Christian Solgaard (csol@space.dtu.dk)

Abstract. The Greenland GNSS Network (GNET) consists of 71 individual geodetic-grade Global Navigation Satellite Systems (GNSS) stations mounted directly in bedrock located along the perimeter of the Greenland Ice Sheet (GrIS). The first continuously running GNSS (cGNSS) station was set up in 1995 and has been running up to date. During the fourth International Polar Year (IPY) 2007-2008, GNET was established with the expansion of 49 stations. As of 2025, the network has expanded to include 19 town sites and 48 remote sites. Over time, the installations have undergone various updates, helping to stabilize and improve the return observations from the network. The original installations were done using Global Positioning System (GPS)-only receivers; these have, with time, been changed to receivers capable of tracking multiple constellations. Operating cGNSS stations in the remote high Arctic is troublesome, giving rise to data gaps and/or downtime for stations in the network. Here we present the most comprehensive dataset from 1995 to 2025, Receiver Independent Exchange Format (RINEX) v2 and/or v3 daily files are now available, see Table B1. Processed daily East-North-Up (ENU) time series for all sites is available at https://doi.org/10.11583/DTU.31397901 Solgaard et al. (2026), and extensive metadata logfiles documenting the entire lifespan of the specific stations can be found here Danish Agency for Climate Data (KDS) (2026). Photos of the stations can be found on. (https://go-gnet.org/) Through a noise characterization analysis, we show that a fractional Gaussian noise profile is expected. Furthermore, we compare our processed ENU time series with already published subsets of the full dataset from independent processing centers. Here, we conclude that the DTU release is significantly more stable in the horizontal components compared to other publicly available products.

https://doi.org/10.5194/essd-2026-198
Preprint. Discussion started: 8 April 2026

Open Access Earth System Science Data Discussions

1 Introduction

Understanding the response of the solid Earth to current and past changes in the Greenland Ice Sheet (GrIS) is fundamental for quantifying mass balance, constraining Glacial Isostatic Adjustment (GIA), and improving projections of sea-level change. Continuous Global Navigation Satellite System (cGNSS) measurements have become indispensable for detecting the elastic and viscoelastic deformation associated with ice-mass variability, e.g., Bevis et al. (2012); Khan et al. (2010); Simpson et al. (2011). To address the need for a high-precision geodetic observation system in this rapidly changing region, the Greenland GNSS Network (GNET) was established as a distributed array of continuously operating geodetic-grade GPS/GNSS stations along the perimeter of Greenland during the 4.th International Polar Year (IPY) (2007-2008). Since its inception, GNET has provided critical constraints for studies of ice-mass changes Khan et al. (2010ab); Kjeldsen et al. (2013); Barletta et al. (2024), elastic displacement and loading signals Liu et al. (2017); Nielsen et al. (2012), longer-term visco-elastic deformation Khan et al. (2016); Berg et al. (2025, 2024), and the sensitivity of the ice sheet to atmospheric forcing Bevis et al. (2019), along with other studies. See the full publication list using data from GNET at (https://go-gnet.org/).

With close to two decades of continuous operation at most GNET sites, it is now possible to perform a comprehensive quality assessment of the network. The aim of this study is to evaluate the performance of each station in terms of daily data-return performance, noise characteristics, and overall stability. In addition, we compare the processed time series with previously published processed ENU time series from the Nevada Geodetic Laboratory (NGL), which performs high-volume processing of international GNSS networks—currently on the order of 17,000 stations daily, which are prone to errors Blewitt et al. (2018)—as well as with time series processed by the Jet Propulsion Laboratory (JPL) Heflin et al. (2020).

The dataset published here provides one of the most complete geodetic records of Greenland's crustal motion as measured by permanent GNSS stations mounted in bedrock. By consolidating all GNET observations within an open, versioned, findable, and citable repository, we aim to;

- Enhance transparency and reproducibility.
- Enable improved integration of GNSS observations with gravimetry, altimetry, and numerical modeling.
- Support the development of refined GIA models, elastic loading, and mass-balance models for Greenland. Khan et al. (2016); Barletta et al. (2024)

This release establishes a robust geodetic reference frame for tracking long-term solid-Earth processes, including lithospheric displacement, regional tectonics, and sea-level-driven loading, in one of the fastest-evolving cryospheric environments on Earth Greene et al. (2024).

With this publication, we present the most comprehensive release of the GNET data archive, which Includes: 1) Raw GPS/GNSS observations spanning the full operational history of the network, plus additional older stations predating GNET, provided in standardized RINEX format; 2) Processed ENU displacement time series, based upon the GypsyX processing methodology; 3) the complete metadata record, including equipment histories, monument details, site geology, data quality,

https://doi.org/10.5194/essd-2026-198
Preprint. Discussion started: 8 April 2026

and return statistics for each station.

In the following sections, we describe the history of GNSS monitoring in Greenland both prior and after the establishment of GNET, including the original and current configuration of GNET. We then detail the data acquisition and processing pipelines, evaluation of the framework stability for each GNSS site. Next, we provide metadata and availability for each site, a comparison with already published time series from other institutions. Finally, we outline the main structure of the released dataset.

1.1 History of GNSS monitoring in Greenland

The primary challenge for the International GPS Service for Geodynamics (IGS) in the mid 1990s was to improve the accuracy of the GPS satellite orbits by increasing the number and geographical distribution of the global tracking network. As an outcome of the IGS meeting in Pasadena 1994, the proposal for extension of the global network was suggested. Based on the suggested expansion of a global GNSS network from IGS in 1994, the first permanent GPS station was established at Thule Airbase (now Pituffik Space Base) in 1995.

During the mid/late 1990'ties national geodetic networks had to be re-measured with GNSS to meet the accuracy potential in GNSS as the global tracking network evolved and processing theory, techniques, and modelling of systematic errors were improved. First of all geodetic datums had to be changed from regional to global, and coordinates had to be realized in a Reference Frame where GPS-derived coordinates from the global tracking network contribute to orbit modelling. Establishment of permanent stations tracking GNSS signals serves two major purposes:

1) Support the international scientific community:

- With data from IGS stations in Greenland to improve GNSS products like orbit and clocks, ionosphere and troposphere models, terrestrial reference frames, etc.
- Reference for various scientific projects, e.g., airborne surveys of gravity, laser, radar, photo missions, etc.

2) Form the basic geometric infrastructure for:

- GNSS-based measurements and definitions of national control networks and territorial base, e.g., Greenland Reference Frame 1996 (GRF96).
- Topographical and nautical maps.
- Positioning of critical infrastructure, e.g., airport runways, navigation instruments, etc.

In the 1990'ties the standard for national geodetic networks went from episodic GNSS campaign surveys between existing survey markers to a fundamental network of permanent GNSS stations monitoring station velocities rather than fixed coordinates. These permanent GNSS stations would then support episodic re-surveys of stations in the national networks, and repeated velocities derived from previous surveys can be compared to velocities from the permanent stations.

https://doi.org/10.5194/essd-2026-198
Preprint. Discussion started: 8 April 2026

Before the GNET projects the plans for a general coverage of Greenland with permanent sites were Thule, Upernavik, Kangerlussuaq, Qaqortoq, Kulusuk, Scoresbysund, Danmarkshavn and Station Nord. During the Reference Greenland Network campaign (1996-2001), this network was used to provide GNSS coordinates to about 100 existing survey markers with coordinates from episodic Transit Doppler or triangulation campaigns. When IGS was formally established in 1994 there were no firm standards for antenna monuments. Standards have developed over time, and early built monuments were, in some cases, replaced with new ones to match up with standards.

1.2 Permanent GNSS stations established prior to GNET (including replacement stations)

THU1: In May 1995, the first IGS station in Greenland was established at Thule Airbase in collaboration with Bob Thomas from NASA/Langley Research Center, who supplied hardware in the form of an Allan Osborne Dorne Margolin T antenna and Rogue SNR-12 receiver. Monumentation was a metal platform attached to the roof of a flattop building, which was founded on three feet active frozen soil layer. **THU2**: In 1998 a new 1.5 m concrete pillar monument (THU2 43001M002) was established on solid bedrock. The pillar was formed as a truncated pyramid with a taper smaller than the chookering antenna diameter. THU2 supported the IGS International GLONASS Experiment IGEX-98, followed by the International GLONASS Service (IGLOS). The antenna was a combined GPS/GLONASS antenna (ASH701073.1), and the receiver was a combined GPS/Glonass Ashtech Z-18. The original antenna was changed to a Leica multi-frequency GNSS antenna (LEIAR20 with a LEIM radome) in August 2025, as the old antenna started to fail. **THU4**: To maintain continuity in station velocities in the IGS time series, a new monument (THU4 43001M003) was established in 2010 to accommodate tracking of multi-frequency GNSS constellations rather than changing the antenna in THU2. The new monument was a 2.5 m concrete pillar shaped as a truncated pyramid. THU4 was built 7 meters north of THU2, and the antenna is at the same height as the THU2 antenna. **KELY**: Kellyville KELY was built in July 1995 on a proposal from Professor John Wahr from the University of Colorado, who wanted to study GIA and viscoelastic solid Earth response from mass balance change of the GrIS. Absolute gravity was measured at regular intervals with the FG5 gravimeter. The project was funded by the National Science Foundation (NSF), and the station was hosted by Stanford Research Institute (SRI). KELY was collocated with a 32m parabola radar antenna for ionospheric studies of the upper atmosphere. The monument is a 1.5 m concrete pillar about 0.5m wide. During the radar's operation, the GPS receiver was disconnected due to conflicting signals in the L-band. In May 2018, the facility's operation ended, and KELY was out of operation until DTU Space, on behalf of the Agency for Climate Data, reinstalled KELY with autonomous power and broadband data transmission in August 2020. When the plans for ending operations at Kellyville became public, DTU Space built a replacement station on Black Ridge near Kangerlussuaq Airport. **KLSQ**: KLSQ was built in June 2014 as a replacement for KELY, which was announced as decommissioned. The monument is a 2.5m concrete pillar shaped as a truncated pyramid. There are about 4 years of data from both stations to transfer time series. **KULU:** Kulusuk KULU was built in June 1996, also on a proposal from Professor John Wahr, to study GIA and viscoelastic solid Earth response to mass changes of the GrIS. In Kulusuk, especially the response from dynamic discharge from the large glaciers with margins in fjords (Helheim-, Fenris-, and Midgårdsgletscher). In Kulusuk, absolute gravity measurements were performed at regular intervals. The monument was an existing camera monument from a former stellar triangulation experiment in the early 1970s.

https://doi.org/10.5194/essd-2026-198
Preprint. Discussion started: 8 April 2026

From the beginning, data were collected on a local PC and sent by ordinary post on floppy discs. Data return was rather poor due to the local power supply and PC problems. In 2023, the receiver was moved to the basement of Hotel Kulusuk to mitigate numerous power outages. **SCOB**: Ittoqqortoormiit (Scoresbysuund) SCOB was established in August 1997. The monument was a modified 3 m steel lamppost with a Trimble 4000 SSi receiver and "TRM29659.00 DOME" antenna. DOME was a custom-made plexiglass semi-hemispherical radome. The operation stopped in 2005. **SCOR**: In 2004, a new 1.5 m concrete pillar monument (SCOR 43006M002) was established about 22 m from SCOR. The pillar was formed as a truncated pyramid. **QAQ1**: Qaqortoq QAQ1 was established in September 2001. The monument is a 2.5m concrete pillar shaped as a truncated pyramid. The antenna has been changed 4 times with GPS-only antennas due to antenna failures. The last antenna change was in 2003. **QEQE**: Qeqertarsuaq QEQE In 2005 a 1.5 m concrete pillar was established on solid bedrock. The pillar was formed as a truncated pyramid. In 2013, the GPS-only antenna was changed to a multi-frequency GNSS antenna. **ILUL**: Ilulissat ILUL was established in 2005 by DTU on behalf of Professor Tonie van Dam from University of Luxembourg. The location was Ilulissat Airport, and only a low monument was allowed. The monument consisted of 3 threaded 12 mm rods drilled into the bedrock. The antenna was mounted on a stainless steel disc. When the station went online, the ownership was transferred to DTU. **AASI**: Aasiaat AASI was established in 2005 by DTU on behalf of Professor Tonie van Dam from the University of Luxembourg. The location was Aasiaat Airport, and only a low monument was allowed. The monument consisted of 3 threaded 12 mm rods drilled into the bedrock. The antenna was mounted on a stainless steel disc. When the station went online, the ownership was transferred to DTU. The operation was stopped in 2023. **AAS2**: was established in 2022. The monument is a 1 m aluminium pipe drilled into the bedrock. This new station was established to take over from the original AASI station; the switch was performed to improve the station's stability with an updated monument. **UPVK**: Upernavik UPVK was established in early 2007 at Upernavik Airport. Monument is a 1 m aluminium pipe drilled into the bedrock. **NORD**: Station Nord. In 2006, a 1.5 m concrete pillar was established in permanently frozen soil that was found 1 meter below the surface. A layer of 0.5 meter frozen soil was removed, and the floor of the excavation was levelled with loose soil. A concrete baseplate (1 x 1 x 0.3 meters) for the pillar was pre-cast in a garage, transported, and lowered onto the floor of the excavation by a backhoe. The baseplate pillar consists of a square part from the base plate to 0.3 meters above the terrain. From here, the pillar was formed as a truncated pyramid. Finally, the terrain was elevated by 0.5 meters around the construction. For further information, we suggest looking into the IGS style logbooks.

1.3 The Greenland GNSS Network (GNET)

GNET was established as part of the Polar Earth Observing System (POLENET) during the 4th IPY Hawley and Brunt (2019). The original goal for the project was to observe and improve the understanding of ice-mass changes of the Greenland ice sheet. The original 58 cGNSS stations was established during three field seasons from 2007-2009 as a collaboration between several groups. The Ohio State University (OSU), the National Science Foundation (NSF), NASA's JPL, UNAVCO (now Earthscope), the University of Luxembourg, and the Technical University of Denmark (DTU). From the initial establishment of the network to 2019 the maintenance and development were shared and coordinated between OSU, UNAVCO, and DTU. As of January 2019, NSF and the Danish agency for data supply and efficiency (SDFE) (now the Danish agency for climate data (KDS))

https://doi.org/10.5194/essd-2026-198
Preprint. Discussion started: 8 April 2026

signed an agreement handing over the ownership of GNET to the Danish government. Since then, the ongoing development and maintenance of the network has been carried out in collaboration between KDS and DTU SPACE Hawley et al. (2017). Since 2019, the network has been expanded further from the original 58 cGNSS stations (including the prior-GNET stations) to a total of 71 stations spread over 67 unique locations, as some stations share the same antenna, see Fig. 1 and Table 1.

2 Network description

The current network consists of 19 unique town sites and 48 remote sites. Of the 19 town sites, 4 of them are classified as IGS GNSS stations International GNSS Service (2026). At some sites, multiple antennas are installed, like THU2 vs THU4, where THU2 is the original antenna, and THU4 is an upgraded version; only the THU2 time series is included here. The current configuration of stations is shown in Fig. 1. When the network was expanded in 2007-2009, the main aim was to recover the PGR and GIA at the major outlet glaciers The Danish Agency for Climate Data (Klimadatastyrelsen) (2026); Hawley et al. (2017). The stations are, where possible, located with an inland site and one further out towards the ocean, to analyze the same effect from multiple distances from the source (Grls).

Table 1: List of the GNET GNSS sites with coordinates, station IDs, location names, date of installation, last valid epoch by January 2026, and station type. For the receiver type and antenna, we refer to the logbooks https://dataforsyningen.dk/data/4804 Danish Agency for Climate Data (KDS) (2026). If no "Last valid Epoch is listed, then the station was operational by the time of publishing. The coordinates in the list match the coordinates in the IGS logs.

Station ID	Location Name	Latitude (°N)	Longitude (°E)	Elevation (m)	Date of Installation	Last valid Epoch	Type	Sampling Rate [s]
AAS2	Aasiaat	68.71937	-52.79321	57.7	2022-08-08	-	Town	1
AASI	Aasiaat	68.71932	-52.79335	56.4	2005-09-28	2023-08-21	Town	1
ASKY	Astrup Kystland	75.72611	-58.25706	699.0	2007-08-19	-	Remote	15
AVAN	Avannarliit	69.10636	-50.99616	460.5	2024-08-19	-	Remote	15
BLAS	Blaasø	79.53861	-22.97438	507.0	2008-07-07	-	Remote	15
DANE	Daneborg	74.31194	-20.19963	196.0	2009-08-15	-	Remote	15
DGJG	Daugaard-Jensens Glacier	71.78653	-29.84986	1517.0	2009-08-11	-	Remote	15
DKSG	Docker Smith Glacier	76.35161	-61.67737	621.0	2007-08-21	-	Remote	15
DMHN	Danmarkshavn	76.77108	-18.65568	55.5	2009-08-20	-	Town	1
EQNU	Eqaluit Nunataat	69.11657	-49.68517	326.3	2024-08-20	-	Remote	15
GMMA	Gamma Ø	77.80943	-19.65188	536.0	2009-08-19	-	Remote	15
GROK	Grønne nunatak	78.44270	-22.90353	1058.0	2008-07-05	-	Remote	15

https://doi.org/10.5194/essd-2026-198
Preprint. Discussion started: 8 April 2026

HEL2	Helheim	66.40115	-38.21540	447.0	2007-08-24	-	Remote	15
HJOR	Hjørnedal	63.41820	-41.14755	784.0	2007-08-13	-	Remote	15
HMBG	Hamberg Glacier	73.67598	-28.12875	1342.0	2009-08-12	-	Remote	15
HRDG	Harder Glacier	81.87983	-44.51714	732.0	2008-07-10	-	Remote	15
ILUL	Ilulissat	69.24042	-51.06076	55.6	2005-09-25	-	Town	1
ISOR	Isortoq	65.54666	-38.97492	83.5	2007-08-22	-	Town	1
JGBL	Jørgen Brønlund	82.20876	-31.00380	775.0	2008-07-09	-	Remote	15
JWLF	Jewell Fjord	83.11166	-45.11961	127.0	2008-07-16	-	Remote	15
KAGA	Kangia	69.22232	-49.81426	169.0	2006-05-23	-	Remote	15
KAGZ	Kap Agassiz	79.13195	-65.85289	97.0	2007-08-29	-	Remote	15
KAPI	Kapisilit	64.43235	-50.27121	104.1	2008-10-01	-	Town	1
KBUG	Køge Bugt	65.14367	-41.15723	312.0	2007-08-27	-	Remote	15
KELY	Kellyville	66.98742	-50.94485	230.0	1995-07-23	-	Remote	15
KLSQ/ KLQ3	Kangerlussuaq Black Ridge	66.99561	-50.62024	353.2	2014-06-02	-	Town	1
KLY2	Kellyville	66.98673	-50.95074	292.9	2020-08-03	-	Remote	15
KMJP	Kap Morris Jessup	83.64325	-33.37690	100.0	2008-07-15	-	Remote	15
KMOR	Kap Morton	81.25272	-63.52714	219.0	2007-09-03	-	Remote	15
KSNB	Steenstrup Nordre Glacier	66.86328	-35.57602	1736.0	2007-08-17	-	Remote	15
KSUT	Kitsissut	64.07070	-52.00770	40.7	2023-08-22	-	Town	1
KUAQ	Kangerlussuaq Glacier	68.58699	-33.05244	884.0	2009-08-06	-	Remote	15
KULL	Kullorsuaq	74.58063	-57.22707	94.1	2007-08-14	-	Town	1
KULU	Kulusuk	65.57934	-37.14936	67.5	1996-06-21	-	Town	1
LBIB	L. Bistrup Glacier	75.89383	-23.85286	1511.0	2009-08-14	-	Remote	15
LEFN	Leffingwell Nunatak	80.45669	-26.29322	705.0	2008-07-03	-	Remote	15
LYNS	Lynaes	64.43047	-40.19775	197.0	2007-08-28	-	Remote	15
MARG	Marie Glacier	77.18703	-65.69433	683.0	2007-08-25	-	Remote	15
MIK2	Mikisfjord	68.14027	-31.45150	836.0	2009-08-07	-	Remote	15
MSVG	Mestersvig	72.24085	-23.91240	111.0	2009-08-10	-	Remote	15
NGFJ	Ingolf fjorden	80.56848	-16.84113	35.5	2024-08-13	-	Remote	5

https://doi.org/10.5194/essd-2026-198
Preprint. Discussion started: 8 April 2026

NNVN	North Niviarsiat Nunatak	61.63188	-44.90073	2150.0	2007-08-14	-	Remote	15
NORD	Station Nord	81.60000	-16.65556	40.0	2006-09-21	-	Town	1
NRSK	Norske Øer	79.15504	-17.72517	362.0	2008-07-04	-	Remote	15
NUNA	Nunatarsuaq	69.20386	-50.45365	229.5	2024-08-20	-	Remote	15
NUUK	Nuuk	64.18355	-51.73116	109.4	2008-10-01	-	Town	1
PAMI	Pamiut	62.01157	-49.67097	99.8	2017-09-01	-	Town	1
PLPK	Pilappik	66.89773	-34.03316	144.0	2007-08-11	-	Remote	5
QAQ1	Qaqortoq	60.71520	-46.04780	74.0	2001-10-15	-	Town	1
QENU	Qeqetaarsunnguit Nunataat	69.11909	-50.46859	428.5	2024-08-20	-	Remote	15
QEQE	Qeqertarsuaq	69.25263	-53.52233	48.8	2005-07-10	-	Town	1
QAAR	Qaarsut	70.74041	-52.68838	53.1	2007-08-28	-	Town	1
RINK	Rink Glacier	71.84848	-50.99373	1358.0	2007-08-26	-	Remote	15
SCBY	Kap Schouby	80.26014	-59.59335	559.0	2007-09-08	-	Remote	15
SCOB	Ittoqqortoormiit	70.48524	-21.95084	128.631	1997-08-07	2005-10-20	Town	30
SCOR/ SCO4	Ittoqqortoormiit	70.48534	-21.95034	128.5	2004-09-07	-	Town	1
SENU	Sermip Nunataa	61.06959	-47.14100	683.0	2008-05-16	-	Remote	15
SISI	Sisimiut	66.93431	-53.67286	112.9	2012-09-24	-	Town	1
SRMP	Sermip Nunataa	72.91066	-54.39342	396.0	2007-08-11	-	Remote	15
THU1	Pituffik Space base	76.53733	-68.78801	55.014	1995-05-02	2003-01-12	Town	30
THU2	Pituffik Space base	76.53711	-68.82495	36.5	1998-10-26	-	Town	1
TIMM	Timmiarmiut	62.53554	-42.28581	331.0	2007-08-19	-	Remote	15
TIN1	Tininilik	68.80124	-50.46319	537.3	2010-05-27	-	Remote	15
TREO	Trefoldigheden	64.27708	-41.37476	144.0	2007-08-31	-	Remote	15
UPAK	Uippak	63.09542	-41.31591	119.9	2024-08-24	-	Remote	5
UPVK	Upernavik	72.78833	-56.12806	165.0	2007-06-02	-	Town	1
UTMG	Timmiarmiit Glacier	62.92721	-43.30609	1489.0	2007-08-19	-	Remote	15
VFDG	Vestfjord Glacier	70.29992	-29.81735	1310.0	2009-08-08	-	Remote	15
WTHG	Walterhausen Glacier	73.95519	-24.30870	1125.0	2009-08-13	-	Remote	15
YMER	Ymer Nunatak	77.43290	-24.32609	1083.0	2009-08-18	-	Remote	15

https://doi.org/10.5194/essd-2026-198
Preprint. Discussion started: 8 April 2026

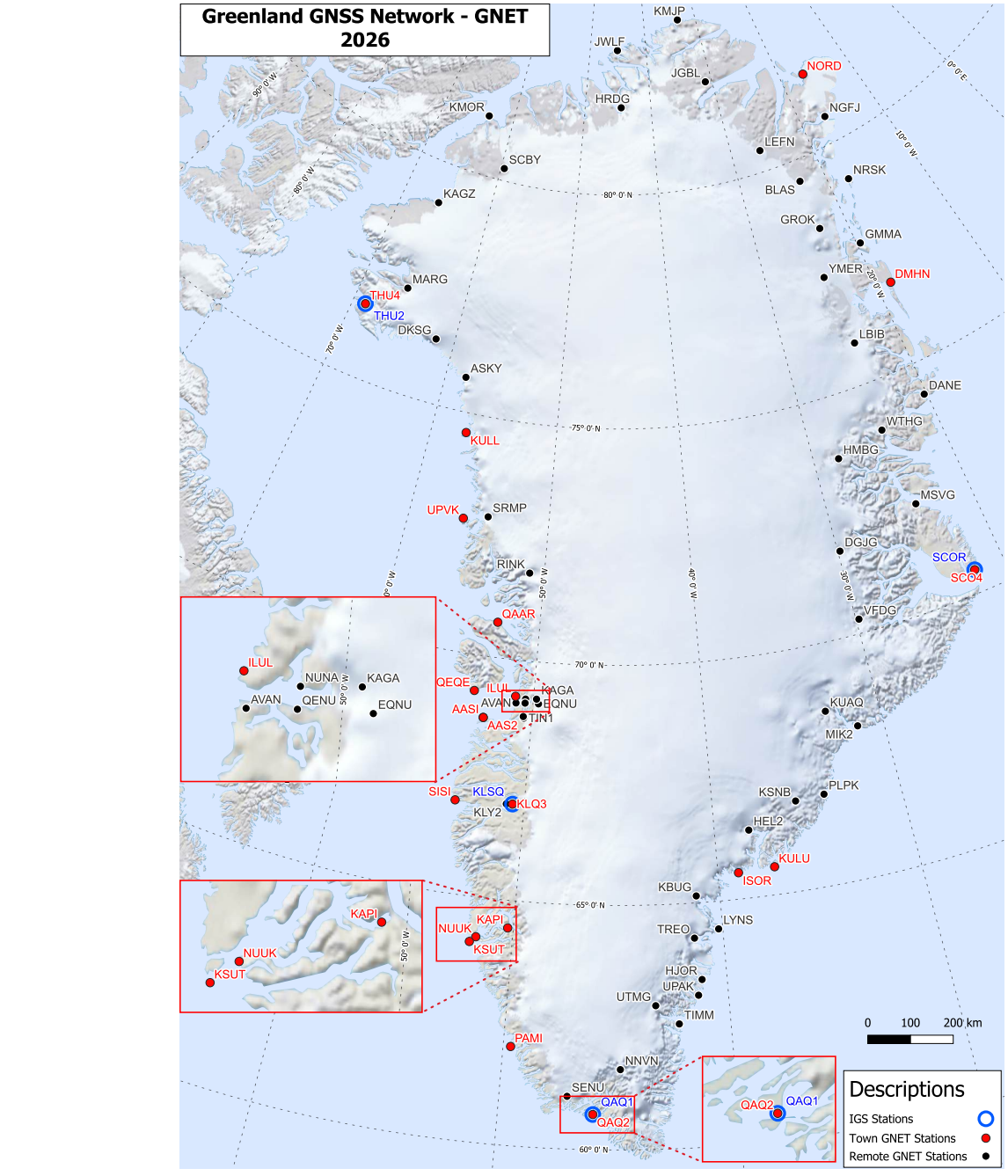

Figure 1. Overview map of the current configuration of GNET. The map was produced using the QGreenland QGIS package Fisher et al. (2023).

https://doi.org/10.5194/essd-2026-198
Preprint. Discussion started: 8 April 2026

2.1 General station description

GNET is built around two main station designs: a town site and a remote site version. The remote sites are all located in hostile and hard-to-access areas of Greenland, with the sites shown in Fig. 1. The remote sites are therefore expected to run autonomously throughout the year. An example of the remote GNET station design is Shown in Fig. 4b and drawn in a simple schematic in Fig. 2a. The station design is based upon the design provided by Earthscope (then UNAVCO) for GNSS network solutions all over the world UNAVCO Inc. (2026). The current configuration of the remote sites includes at most sites a Leica AR20 GNSS antenna, an AlertGEO Resolute GNSS receiver Xeos Technologies Inc. (2024) and various hardware for charging the up to 24 100Ah lead-acid batteries using solar panels mounted on a frame. Communication to and from the remote sites is either through Iridium or, for stations in closer proximity to towns/settlements the local broadband connection. This constellation provides the operational team with the opportunity to retrieve state-of-health messages: battery voltage, internal temperatures, number of GNSS satellites tracked, etc. Used for determining the status of the stations throughout the year. The stations can also be updated or powered up/down remotely to avoid data loss or permanent damage to the battery-pack, if the voltage starts dropping below the Low-Voltage-disconnect (LVD) threshold value of 11.3V during the winter months. The antenna monument installations vary with minor deviations from site to site. Common for all sites is that the monument is bolted into, or cast in concrete on top of the stable bedrock.

The 19 town sites included in the network are built around a different framework. These sites are all connected to the main electrical grid, removing the need for a low-power system. An example of a town site QEQE is shown in Fig. 4 and shown in schematic in Fig. 2. The current configuration consist of an enclosure, either a pelicase like box (QEQE and QAAR) or a metal enclosure made for installation inside a building. The enclosure holds all the electronics for the station: A Septentrio PolaRx5 GNSS receiver Septentrio (2025), A UPS system, a black box, and WiFi modem. This setup helps ensure a stable connection and time series from each site. Over the years, the town sites have shown to be more unstable than the remote sites. This is mainly due to a power or data connection loss. The main grid has not been shown to be as stable as the battery bank solution used at remote sites. For a detailed description of the instrumentation history for each site, we encourage the reader to read the IGS logbook for the specific site Danish Agency for Climate Data (KDS) (2026).

2.2 Station design and maintenance

All stations are, on average, visited by a field crew from DTU Space and/or KDS once a year, with the remote sites being prioritized compared to the town sites. This maintenance round takes place in August every summer, in a helicopter-based operation. It has been the experience that the stations can run autonomously, but without checkups and updates, the harsh climate will destroy the equipment. In addition to the harsh Arctic climate, most of the remote stations have been visited by animals, mostly Polar Fox and Polar Bear. It is the operational teams experience that the smell of petroleum attracts the animals, which means that cables, antennas, boxes, and so on have been attacked over the years. In extreme cases, this has caused a loss

https://doi.org/10.5194/essd-2026-198
Preprint. Discussion started: 8 April 2026

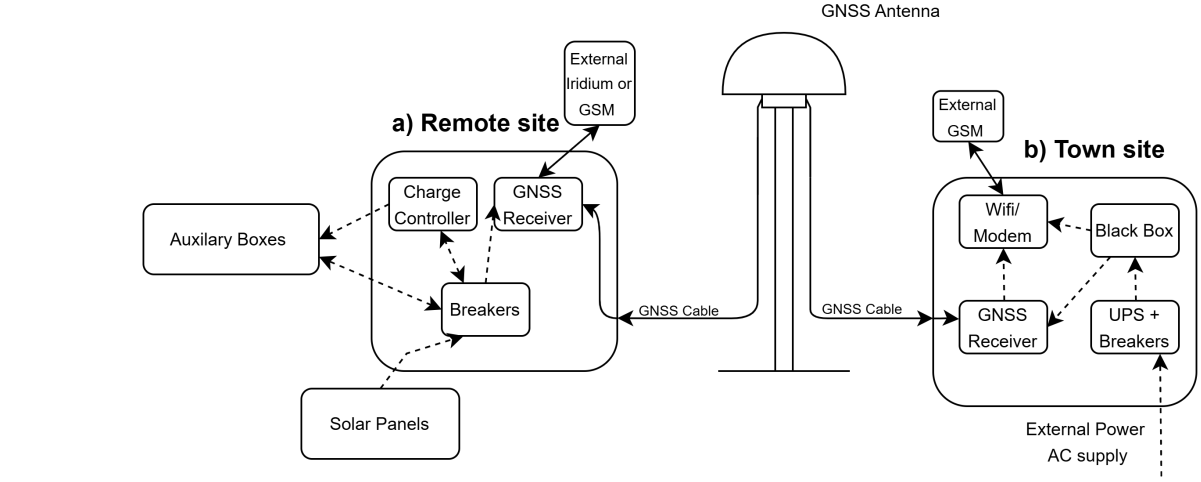

Figure 2. Schematic drawing of a standard town (b) and remote site (a) setup.

of data due to a destroyed or missing antenna. Over the years, all the most affected sites have been protected with metal tubes, metal sheets, and rocks. The yearly maintenance for a remote station includes: checkup of the monument stability, the antenna stability, the frame stability, missing or destroyed solar panels, a checkup of the battery status for all individual batteries, cable test of the GNSS cable, and general firmware updates if needed. Along with this, pictures are taken and archived for each station for each year. .

2.3 Antenna Monument Design

Across GNET, different designs of antenna monument are used. The design of the monument has changed over the years, from the first concrete monument types like KULU (see Fig. 3d) to the newest iteration (see Fig. 3b). The design of the monument is a critical factor in the geodetic quality assurance of a GNSS site, as the monument must be stable and mounted directly to the bedrock. This ensures that the motion of the GNSS antenna only reflects the movement of Earth's crust and minimizes the effect from non-lithospheric motions near the surface International GNSS Service (IGS) (2023). Furthermore, the monument should ensure that the antenna is placed horizontally and can be adjusted to orientation towards true north. To minimize the effects of multipath error, the base of the monument should not be wider that the base of the chokering antenna. The sites KULU and KELY were establish before the monument requirement was implemented for the network. Four different monument designs are used for GNET, examples is shown in Fig. 3. The bedrock-bolted plate monument in 3a and the wide concrete monument in 3d are only used at three sites. For most remote GNET sites the bedrock-bolted mast shown in Fig. 3b or an older version based on the same design philosophy is used. The tall concrete monuments Fig. 3c are only used for town sites. For some town

https://doi.org/10.5194/essd-2026-198
Preprint. Discussion started: 8 April 2026

Figure 3. Comparison of the most common antenna monuments used in GNET. a) bedrock-bolted plate (ILUL). b) bedrock-bolted mast (NGFJ). c) concrete monument (KLSQ). c) older version of the concrete monument (KULU). Pictures Thomas H. Nylen and Christian Solgaard

sites a 2m tall bedrock-bolted mast type is used instead of the concrete monument. The concrete mast monument type, is the most stable option, but due to logistics it is not possible to setup in the field.

The specific locations of GNET sites, are chosen to avoid heavy drift of snow and to reduce the amount of nearby topography 5° over the horizon line of the antenna.

2.4 GNSS Receivers

The current configuration of GNSS receivers is the Septentrio PolaRx5 Septentrio (2025) and the AlertGeo Resolute Xeos Technologies Inc. (2024), both receivers are multi-frequency GNSS reference receivers, built upon the same AsteRx-m2 OEM board. The PolaRx5's are used in town sites, and the Resolute's are used in remote sites. All the PolaRx5 receivers are set to track all constellations/signals except SBAS and log hourly 1Hz SBF files. The Resolute receivers are set to track all signals from GPS and Galileo except for the E6. Due to limited power and file storage room, the logging for most remote sites is set at hourly 15s SBF files. Some remote GNET sites are set to log hourly 5s files; these stations are: PLPK, KAGZ, NGFJ, and UPAK. These stations are used and tested for potential use cases in GNSS-IR applications. Larson et al. (2013)

3 Data processing

The GNET data are processed as a daily product using the GipsyX-2.4 software package Bertiger et al. (2020). We use the final orbit products by JPL, which include satellite orbits, satellite clock parameters, and Earth orientation parameters. The orbit products take the satellite antenna phase center offsets into account. The atmospheric delay parameters are modeled using the Vienna Mapping Function 1 (VMF1) with VMF1grid nominals Boehm et al. (2006). Corrections are applied to remove

https://doi.org/10.5194/essd-2026-198
Preprint. Discussion started: 8 April 2026

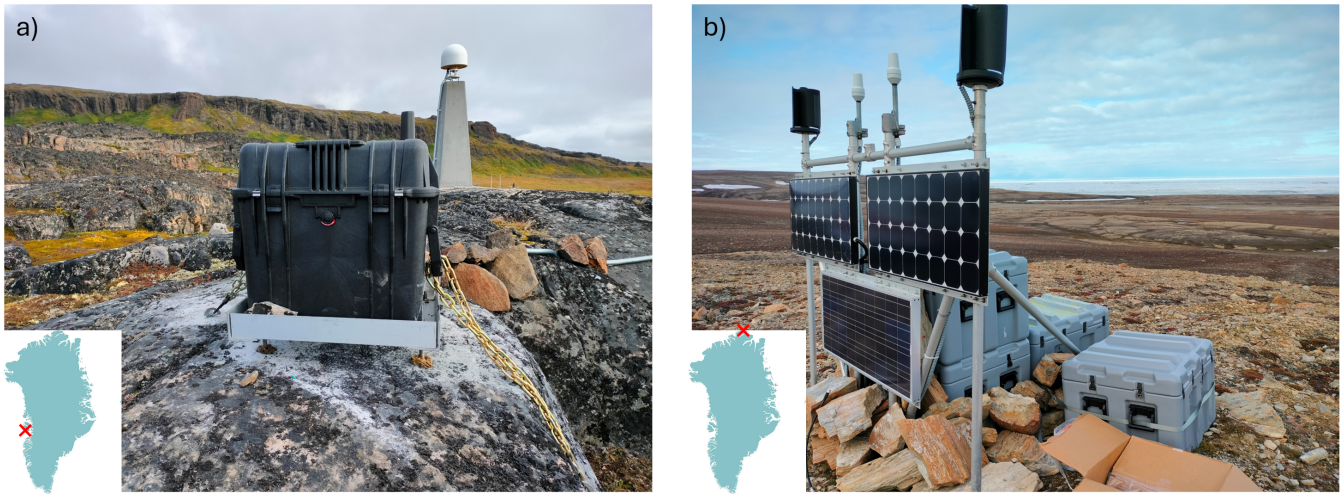

Figure 4. a) The town site QEQE just outside of Qeqertarsuaq on Disko Island in Vest Greenland. The enclosure is provided with power from the town grid, connection is through a GSM antenna placed on top of the pelicase, current receiver type across all town sites is the Septentrio PolaRx5 GNSS receiver Septentrio (2025). b) The remote site KMJP at Kap Morris Jessup, North Greenland. The power is provided by up to four solar panels and a total of up to 24 100Ah lead-acid batteries in the MM36 pelican cases, depending on latitude. Communication is through the Iridium network; the current receiver across all remote sites is the AlertGEO Resolute GNSS receiver Xeos Technologies Inc. (2024). Pictures: Christian Solgaard

the solid Earth tide and ocean tidal loading. The amplitudes and phases of the main ocean tidal loading terms are calculated using the Automatic Loading Provider (https://barre.oso.chalmers.se/loading/l.php) applied to the FES2014b ocean tide model Carrére et al. (2016), including a correction for the center of mass motion of the Earth due to the ocean tides. The time series were processed in the IGS20 reference frame Altamimi et al. (2023). We use the Precise Point Positioning (PPP) processing strategy. All coordinates are estimated in the center-of-mass frame and subsequently transformed to the center-of-figure (CF) frame by subtracting the geocenter motion. To reproduce the time series processed in this study using the GipsyX-2.4 software package and the gd2e.py code, we provide the input file ppp_0.txt, which corresponds to the default static PPP processing tree for GNSS data in gd2e.py.

4 Dataset overview

The dataset we publish here includes the raw daily RINEX format files for all stations in the network and stations prior to the network establishment. The sampling rates differ between town-, remote-sites, and over time due to hardware and power limitations of the network instrumentation. In addition to the raw RINEX files, metadata in the form of IGS-style logfiles and horizon pictures are published. The processed time series are available as daily solutions with associated error estimates in ENU-transformed time series. The processed ENU time series has been reduced to a common reference epoch of January 1st, 2010, 00:00 UTC+0. The reference geodetic coordinates for each station are listed in the associated sumfiles also

https://doi.org/10.5194/essd-2026-198
Preprint. Discussion started: 8 April 2026

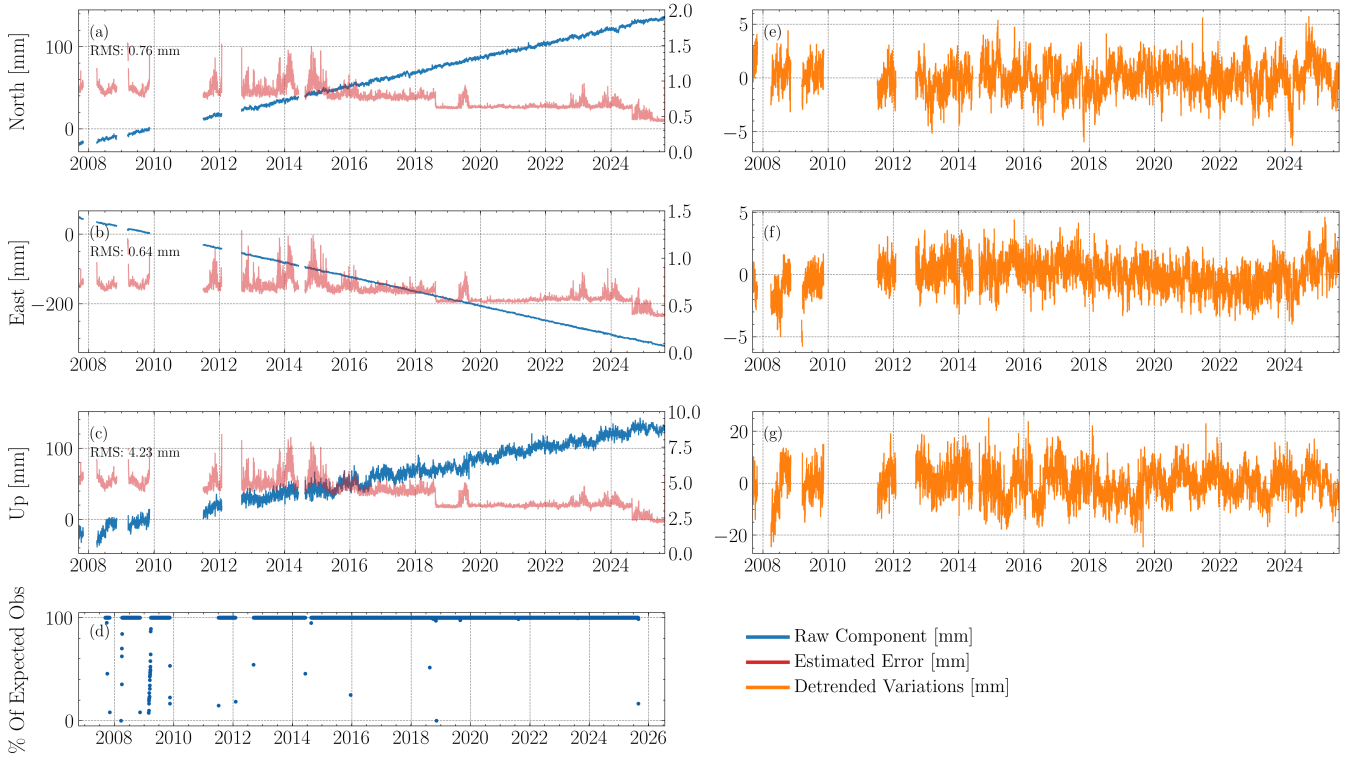

Figure 5. Time series of final processed ENU for station SCBY (Kap Scouby) in Northwest Greenland and the associated error estimates for each coordinate component. a) north component, b) east component, c) up component, all represented in [mm], in reference to the starting coordinate as specified in the metadata for the station. Notice the different scales on the left- and right-hand y-axes. The right y-axis shows the error estimates of the PPP solution. The time series are provided as a daily product. d) shows the % of expected observations for the site, normalized to a sampling rate of 15s. The station results shown here correspond to the IGS logbook visualized in Fig. 9. e-g) Short term variations for each component, derived by removing the linear trend from each component shown in a-c).

published here. An example for the station SCBY (Kap Schouby), a remote GNET site in Northwest Greenland, can be seen in Fig. 5. Here, the ENU time series are displayed along with the associated processing error estimates and the daily return of expected observation. The corresponding IGS-style logfile is visualized in Fig. 9. Along with the processed position time series we provide the derived horizontal and vertical linear velocities with uncertainties. This dataset is visualized in Fig. 6, and summarized in Table A1. The absolute direction of the horizontal displacement shows a general northwest motion for all of Greenland.

4.1 Data Coverage

Operating any kind of continuously running electronics in the Arctic, will at some point cause problems and downtime. Through iterative updating of the station framework, the downtime has been lowered to a minimum as shown in Fig. 7. Both the harsh

https://doi.org/10.5194/essd-2026-198
Preprint. Discussion started: 8 April 2026

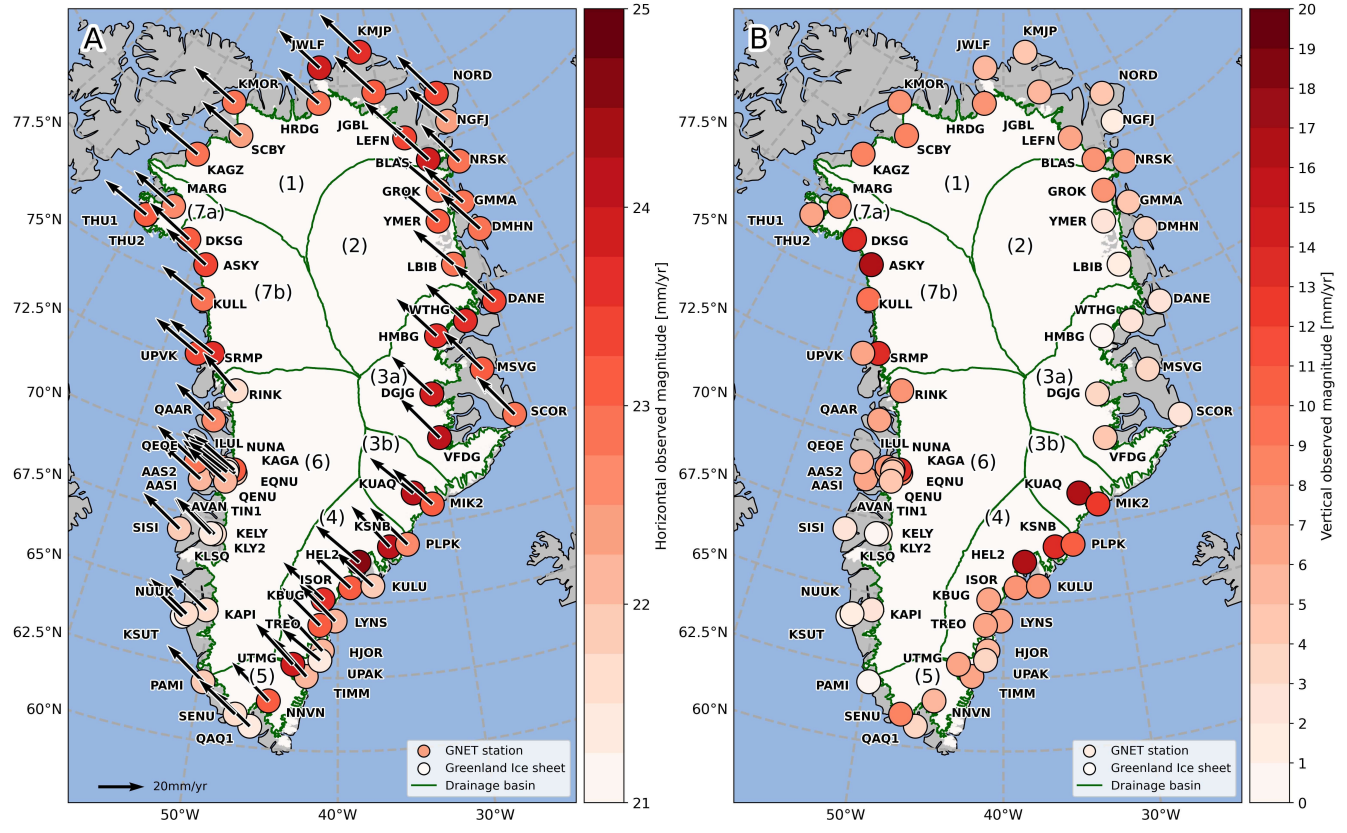

Figure 6. Derived horizontal and vertical linear motion from GNET measurements from 1995 - 2025. The uncertainty for the new stations (see Table 1) will be of a magnitude larger than the older installations, see Table A1. A) Horizontal observed magnitude with absolute direction indicated as arrows, values provided in [mm/year]. B) Vertical observed magnitude given in [mm/year]. For further information on the vertical and horizontal land motion of Greenland see Berg et al. (2024, 2025)

Arctic climate with low temperatures and heavy snowfall, and potential damage by animals have resulted in data gaps during the 20+ years of the project. Typically, foxes and polar bears have been biting through external GNSS cables, iridium antennas, and destroying the solar panels, greatly reducing the performance of a remote site. The full data availability with description of tracked GNSS constellations is shown in Fig. 8.

Fig. 7a) shows the average data return across the network throughout its lifetime. The data return average is normalized to match a 15s sampling rate. With upgrades to the town site enclosures, including the introduction of Black Boxes and UPS systems, and the general receiver change across all sites to the more reliable Septentrio PolaRx5s, the data return has stabilized at around 95-99.9% since 2021. The data return fluctuated substantially in the first years of the network; this is largely due to faulty equipment.

https://doi.org/10.5194/essd-2026-198
Preprint. Discussion started: 8 April 2026

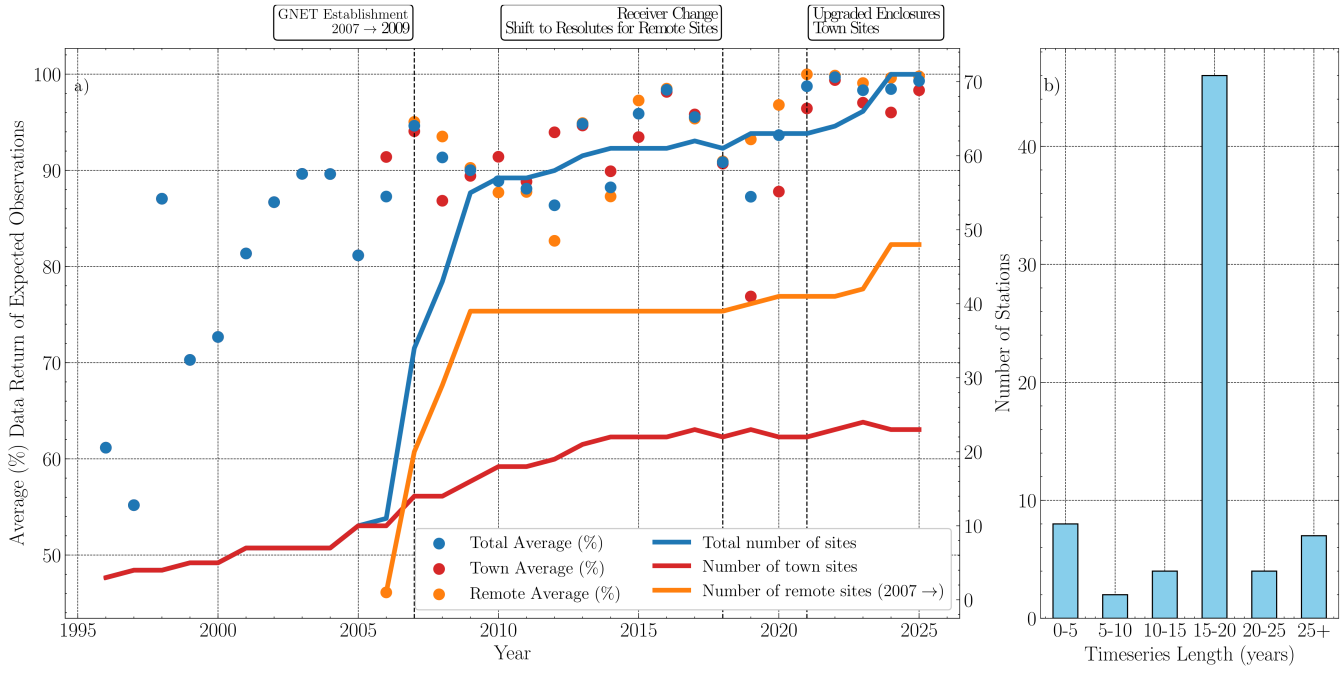

Figure 7. a) Left y-axis: Average data return [%] of expected observations pr. day, normalized to a sampling rate of 15s over the full network. Right y-axis: Total number of stations in the network, split into remote and town sites. The remote sites were first established during the establishment of GNET in the 2007-2009 summer seasons. Some town sites predate GNET back to 1995 (KULU). In 2024, the number of remote sites was expanded with 6 new sites: one in East Greenland (UPAK), one in North East Greenland (NGFJ), and four in the Icefjord area from Ilulissat towards Sermeq kujalleq (NUNA, AVAN, EQNU and QENU). b) Length of the time series distributed over the number of stations in the network.

4.2 Meta Data

For each site in the network, an IGS log is prepared and updated continuously throughout the station's lifetime. Included in the site's logs is information regarding the station configuration over time, as represented in Fig. 9. The visualized logfile here is from the remote GNET site SCBY in Northwest Greenland. The logfile representation corresponds to the final time series product shown in Fig. 5. Notice here, the abrupt change in variability for the error estimations, before and after the receiver change from the Trimple NetRS to the AlertGEO Resolute in summer 2018. The rise in the uncertainty around 2019 corresponds well to the old Ashtech antenna (GPS only) failing and being replaced with the current Leica AR20 (GNSS) antenna. With the receiver change in 2018, it also became a possibility to track Galileo as well as GPS, also contributing to a more stable position solution. Along with the logfiles, images are taken of the stations during the summer maintenance campaign; these are not included in the dataset publication but can be forwarded on demand, upon contact with the corresponding author.

https://doi.org/10.5194/essd-2026-198
Preprint. Discussion started: 8 April 2026

Open Access Earth System Science Data Discussions

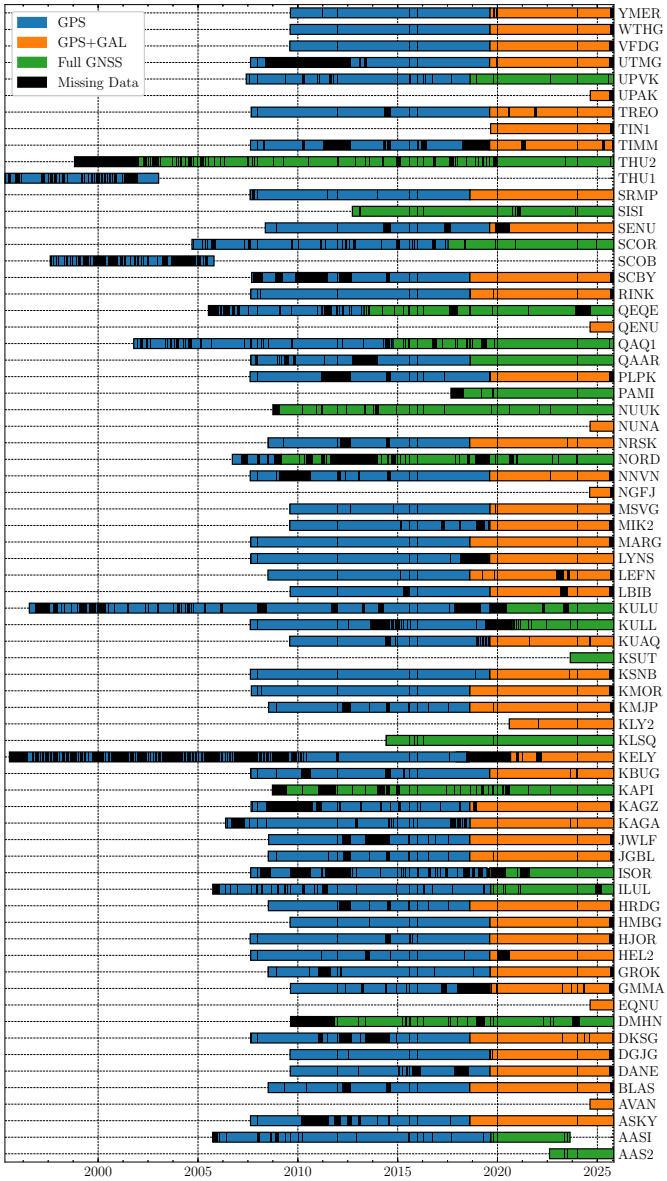

Figure 8. Data availability and overview of the tracked GNSS constellations for each GNET site included in the dataset. Black bars indicate missing data from the processed time series. THU1, SCOB and AASI has all been decommissioned.

https://doi.org/10.5194/essd-2026-198
Preprint. Discussion started: 8 April 2026

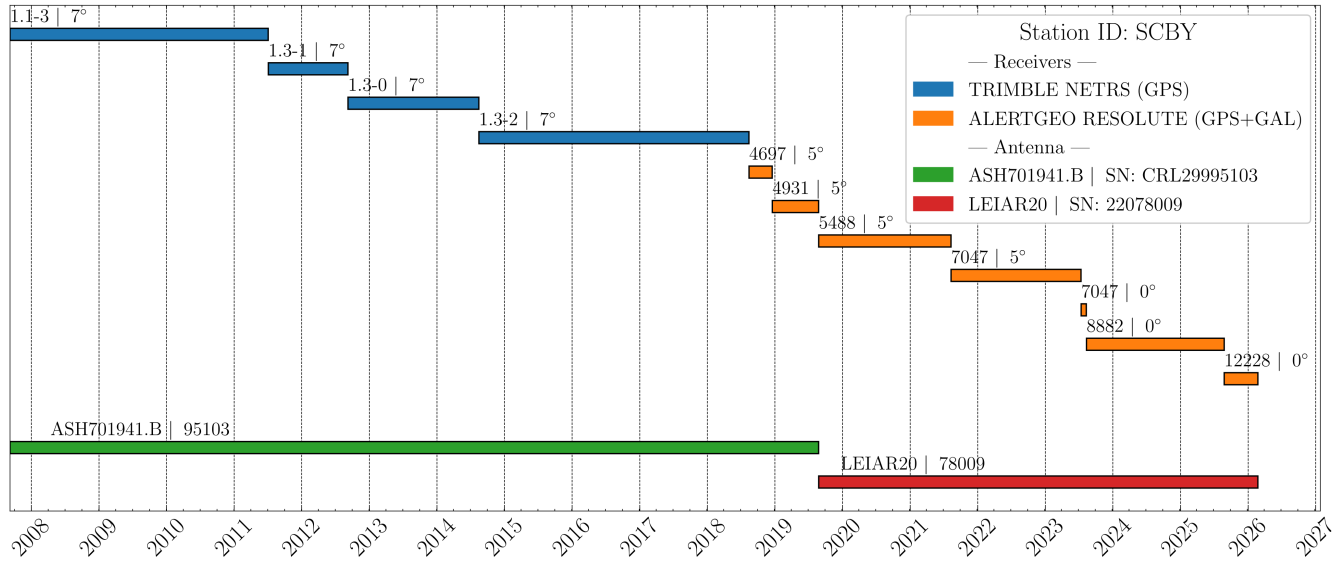

Figure 9. Representation of the IGS sitelog of station SCBY. Information for receivers is "Firmware Version | "Elevation Cutoff Angle" and the antenna information is "Antenna Model" | "Short Serial Number", the station sitelog shown here corresponds to the final ENU time series shown in Fig. 5.

4.3 Dataset evaluation and known limitations

We have chosen to perform two different independent examinations/validations of the stability and quality assurance of the published time series. A stability analysis of the station infrastructure is performed, by estimating the noise characteristics based on a Lomb-Scargle periodogram-derived spectral index Goudarzi et al. (2015). Secondly, we evaluate the published dataset by comparing it directly to already published subsets of the dataset provided by two independent processing centers.

4.3.1 Noise Profile Characteristics

To evaluate the performance of each cGNSS station in the network, a stability analysis is performed. The aim of the analysis is to compute the spectral indices for a power law process fitted to the residual time series for each coordinate component. The power law process is given by:

$$P(f) = P_0(f/f_0)^{\kappa} \tag{1}$$

Where f is the spatial or temporal frequency, P_0 and f_0 are normalized constants, and κ is the spectral index Goudarzi et al. (2015). The spectral indices describe the type of overall noise model. The values of the spectral indices are expected to fall within $-3 < \kappa < 2$ where $\kappa = 0$ defines Gaussian noise, $\kappa = -1$ defines flicker noise, and $\kappa < -1$ defines fractional to random walk noise. Indicies between $-1 < \kappa < 1$ are defined as fractional Gaussian; this is the range we would expect a geodetic grade cGNSS station to lie within. Goudarzi et al. (2015); Montillet and Bos Editors (2020).

https://doi.org/10.5194/essd-2026-198
Preprint. Discussion started: 8 April 2026

The residual ENU time series is computed by fitting and removing a deterministic trajectory model from each component. During the processing, the coordinate estimates are corrected for potential discontinuities due to hardware changes on the stations. A simple model based on a linear trend, annual and semi-annual signal terms are therefore used Montillet and Bos Editors (2020); Bevis and Brown (2014)

$$y(t_i) = a_0 + a_1 t_i + \sum_{j=1}^{n_F} s_j \sin(\omega_j t_i) + c_j \cos(\omega_j t_i) + \epsilon_i \tag{2}$$

Where a_0 is the y-intercept, a_1 is the linear trend, n_F goes to two, such that s_1 and c_1 represent the annual signal and s_2 and c_2 represent the semi-annual. ω is the period set to $\omega_1 = 2\pi/365.25$ and $\omega_2 = 4\pi/365.25$, ϵ is the errors associated with the coordinate estimates, assumed to be Gaussian and uncorrelated. Then for all positions it should be true that:

$$\mathbf{d_{model}} = \mathbf{Gm} + \epsilon \tag{3}$$

Where $\mathbf{d}$ is the data vector, $\mathbf{G}$ is the system design matrix, $\mathbf{m}$ are the model parameters, and ϵ are the associated data errors. The model parameters can then be estimated using the solution for the weighted linear least squares problem given by Aster et al. (2004); Buchta et al. (2025):

$$\mathbf{m} = (\mathbf{G}^{\mathrm{T}}\mathbf{C}^{-1}\mathbf{G})^{-1}\mathbf{G}^{\mathrm{T}}\mathbf{C}^{-1}\mathbf{d} \tag{4}$$

Where $\mathbf{C}$ is the covariance matrix based on the associated error estimates $\mathbf{C} = \mathrm{diag}[\epsilon]$. The deterministic trajectory model is then removed from the ENU time series, which yields a residual time series for each component. We exclude stations with a lifespan of less than 10 years from the analysis. Fig. 10 shows an example of the process, of the upward displacement for the station LEFN (Leffingwell Nunatak), in Northeast Greenland. The resulting Lomb-Scargle Periodogram yields a power law spectral index of $\kappa = -0.67$. The same analysis is carried out for all coordinate components for each station in the network. Fig. 11 shows the final estimated spectral indices across all stations for each coordinate component. The analysis shows that the median spectral index for all components across the full network falls within the range of the fractional Gaussian noise profile.

4.3.2 Comparison to the processed time series by NGL and JPL

A comparison with previously published independent GNSS time-series products is conducted to verify the stability and quality of the full dataset we publish here. We compare and validate the results from DTU with data products from NGL Blewitt et al. (2018) and JPL Heflin et al. (2020). This is done in order to investigate potential differences in longterm linear trends and/or differences in the seasonal signal. NGL's "living dataset" consists of Cartesian coordinate time series from around 17.000 GNSS stations worldwide, of which 10.000 are continuously updated on a weekly basis. The processing is performed using the GipsyX software Bertiger et al. (2020), utilizing JPL orbit and clock parameters. The product is provided as a daily GPS-only-based Cartesian (X,Y,Z) coordinate time series. So, a conversion to the ENU format is performed before the comparison Seeber (2003). We refer to the web page (https://geodesy.unr.edu/, last accessed 22 December 2025) for further information on

https://doi.org/10.5194/essd-2026-198
Preprint. Discussion started: 8 April 2026

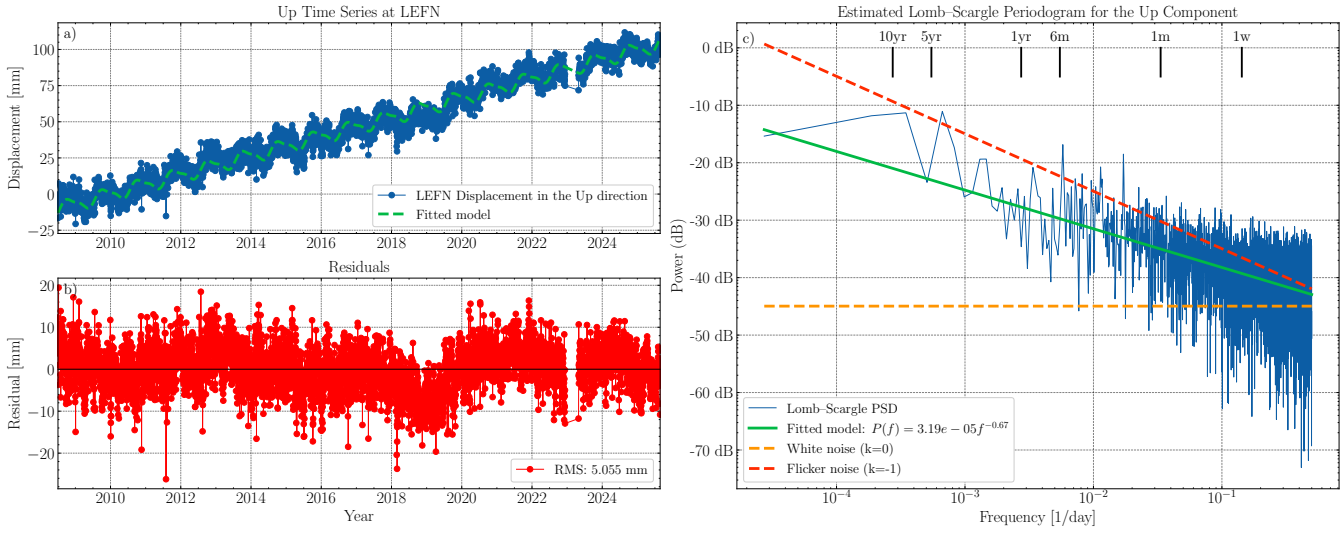

Figure 10. Example of fitting and removal of the deterministic trajectory model and evaluation of the Lomb-Scargle Periodogram. a) Up component from station LEFN and fitted model. b) Corresponding residual time series after the removal of the model. c) Evaluated Lomb-Scargle Periodogram and the fitted power law model for estimation of the spectral index.

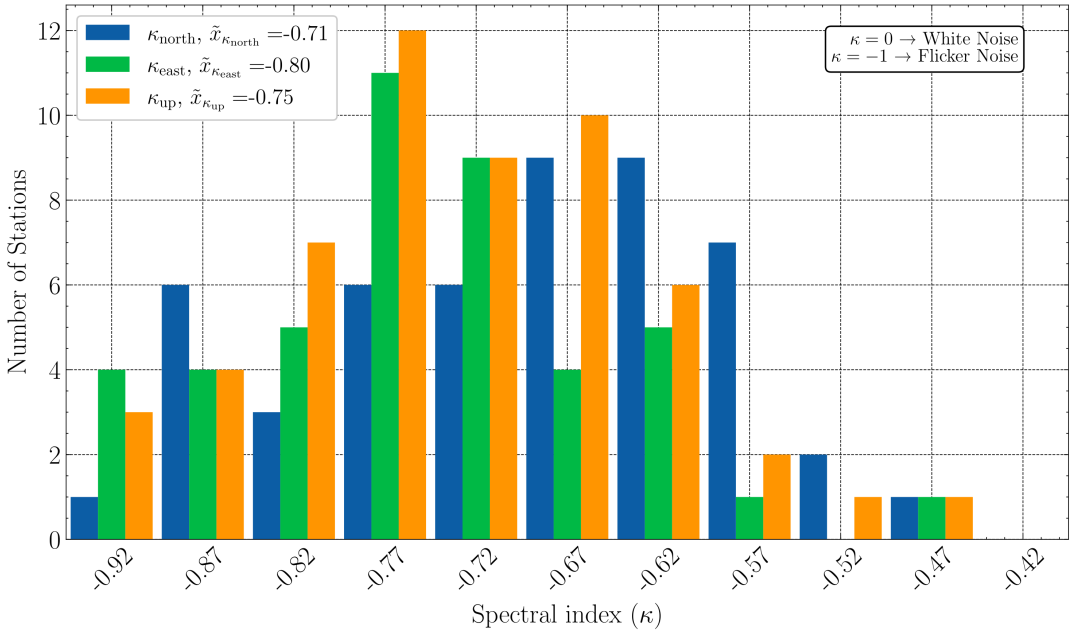

Figure 11. Spectral index κ histogram, of all stations included in the published dataset.

https://doi.org/10.5194/essd-2026-198
Preprint. Discussion started: 8 April 2026

the processing scheme from NGL.

The processed time series from JPL is part of their global archive of processed cGNSS time series NASA Jet Propulsion Laboratory (2018). JPL also uses the Precise Point Positioning (PPP) processing scheme implemented in GipsyX Bertiger et al. (2020); Heflin et al. (2020). The processed time series are provided in both Cartesian and local reference frame ENU format.

To ensure consistency in the comparison, we restrict the analysis to stations common to all three datasets, resulting in 39 of the 71 sites (54%) presented in this study. The lengths of the time series provided by the three data centers are not equal; the processed time series from JPL are, in general, shorter than those for NGL and DTU, which could lead to a bias in the final conclusion. The comparison is performed by fitting the model given in Eq. 2 and extracting the model parameters $\boldsymbol{m} = [a_1, s_1, c_1, s_2, c_2]$ for each coordinate component across all stations. From the model parameters we then compute the linear trend (a_1), the annual amplitude and phase:

$$A_{annual} = \sqrt{s_1^2 + c_1^2},\ \phi_{annual} = \arctan(s_1, c_1) \tag{5}$$

And the semi-annual amplitude and phase:

$$A_{semi-annual} = \sqrt{s_2^2 + c_2^2},\ \phi_{semi-annual} = \arctan(s_2, c_2) \tag{6}$$

We then compare the consistency between the three datasets by fitting a linear model to pair-wise linear trend, annual/semi-annual amplitude and phase, giving us a total of 9 metrics for each parameter. If the trend of the fitted linear model is $\alpha = 1$, then we have a perfect fit and should have consistency across the two datasets for the given parameter. This analysis is shown in Fig. 12 for the annual amplitude of the seasonal signal, along with the fitted model (red line), is a representation of a linear model with trend $\alpha = 1$ and an arbitrary starting point. The computed trends for all pair-wise comparisons with associated R^2 values are presented in Table 2

Comparison of the DTU-processed GNSS time series with products from NGL and JPL reveals good agreement in long-term linear trends across all three processing centers, with slopes near unity ($\alpha \sim 1$) and $R^2 \geq 0.99$ for the north and east components. Vertical trends are slightly less consistent, particularly between DTU and JPL ($\alpha = 0.94$, $R^2 = 0.90$), but this could be biased by the shorter time series provided by JPL.

For the seasonal signals, the amplitude and phase show contrasting results. The amplitude of the annual seasonal signal corresponds roughly in the up direction across the three data sets. However for the horizontal components, almost no correlation is to be found between DTU and NGL $\alpha_{north} = 0.13$ and $\alpha_{east} = 0.10$ it is more consistent for DTU-JPL at ($\alpha_{north} = 0.74$ and $\alpha_{east} = 0.71$, both results combined with the annual phase and the semi-annual seasonal signals show a clear non-zero seasonality in the datasets provided by NGL and JPL which is not found in the data set from DTU. Seasonal displacements in crustal motions in Greenland are expected to be dominated by vertical motion, with only minor horizontal components White et al. (2022); Bian et al. (2023); Materna et al. (2021). The correlation with DTU's product is weak ($R^2 \lesssim 0.5$) and the amplitude of the signals are very low, suggesting these signals are likely processing artifacts from the PPP processing

https://doi.org/10.5194/essd-2026-198
Preprint. Discussion started: 8 April 2026

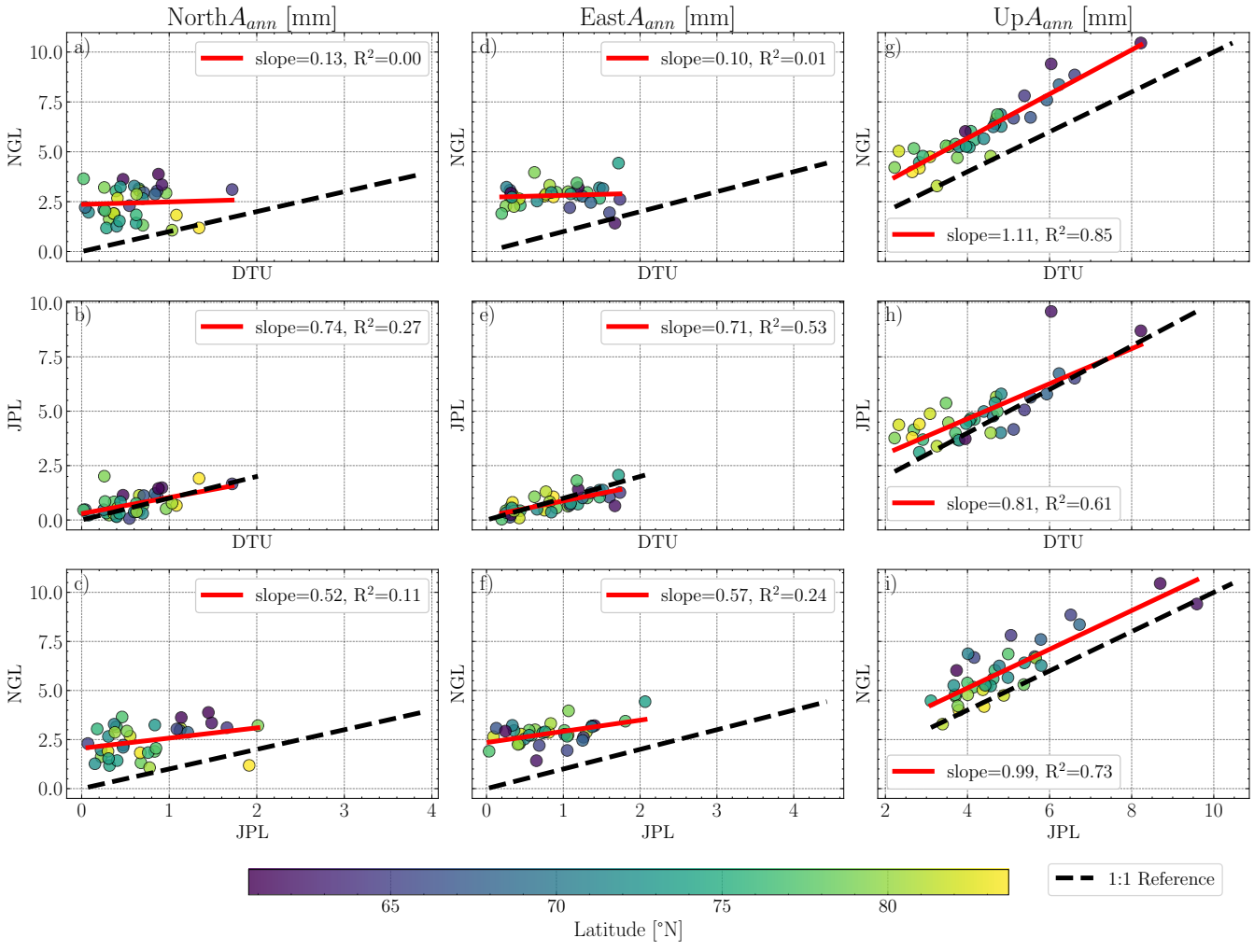

Figure 12. Comparison of the computed annual amplitude of the periodic signal for all coordinate components across the three datasets. a-c) north component (a: NGL vs. DTU, b: JPL vs. DTU, c: NGL vs. DTU). d-f) east component (d: NGL vs. DTU, e: JPL vs. DTU, f: NGL vs. DTU). g-i) up component (g: NGL vs. DTU, h: JPL vs. DTU, i: NGL vs. DTU). The sites are color-coded based upon the latitude of the station.

https://doi.org/10.5194/essd-2026-198
Preprint. Discussion started: 8 April 2026

Metric	Component	$\alpha_{NGL-DTU}$	$R^2_{NGL-DTU}$	$\alpha_{JPL-DTU}$	$R^2_{JPL-DTU}$	$\alpha_{NGL-JPL}$	$R^2_{NGL-JPL}$
Trend	**N**	1.00	1.00	0.99	1.00	1.01	1.00
	E	1.01	1.00	1.00	0.99	1.00	0.99
	U	1.00	0.99	0.94	0.90	0.99	0.94
Annual	**N**	0.13	0.00	0.74	0.27	0.52	0.11
Amplitude	**E**	0.10	0.01	0.71	0.53	0,.57	0.24
	U	1.11	0.85	0.81	0.61	0.99	0.73
Annual Phase	**N**	0.38	0.05	0.19	0.02	0.35	0.11
	E	-0.10	0.01	0.49	0.15	-0.35	0.19
	U	0.68	0.61	-1.30	0.15	-0.02	0.01
Semi-annual	**N**	0.53	0.08	0.54	0.04	0.53	0.60
Amplitude	**E**	0.37	0.07	1.19	0.56	0.42	0.22
	U	0.63	0.25	0.79	0.33	0.29	0.10
Semi-annual Phase	**N**	0.46	0.09	0.97	0.46	0.23	0.05
	E	-0.25	0.09	0.54	0.19	0.12	0.03
	U	0.96	0.98	0.72	0.53	0.74	0.56

Table 2. Combined overview of inter-metric comparison of modeled trends, annual, semi-annual amplitude, and phase for the 39 common found GNET stations in the processed ENU time series provided by the three processing centers (DTU, NGL, and JPL).

choices, reference frame handling, or noise propagation. Consequently, while the vertical seasonal signals can be interpreted confidently, horizontal seasonal amplitudes and phases should be treated with caution when using time series from NGL or JPL.

5 Code and data availability

Information on the GipsyX GNSS analysis software used to process the time series is available here Bertiger et al. (2020). Along with the published dataset, we provide the processing methodology file ppp_0.txt, for reproduction of the processed time series, see Sec. 3. The full post-process noise and stability analysis was conducted in Python, and we refer to https://github.com/CSolgaard/GNET_data_paper_2026 for the source code.

5.1 Raw- and meta-data

The dataset showcased in this study comprises multiple parts. The processed ENU time series is available at https://doi.org/10.11583/DTU.31397901 Solgaard et al. (2026) along with the sum files from the processing, see Sec. 5.2 for further information on the data structure. We refer to Table B1 for a combined overview of the raw RINEX format files. The RINEX data are available as daily files, with sampling rates varying by station type and the year of download.

https://doi.org/10.5194/essd-2026-198
Preprint. Discussion started: 8 April 2026

Table 3: Dataset DOI's/links and citation overview.

Dataset	DOI/Links	Citation
Processed Positional time series and sumfiles	https://doi.org/10.11583/DTU.31397901	Solgaard et al. (2026)
IGS style logfiles	https://dataforsyningen.dk/data/4804	Danish Agency for Climate Data (KDS) (2026)
Daily RINEX files	See Table B1	See Table B1

5.2 Processed positional time series

The individual processed files for each station have been merged into a NetCDF file named `GNET_2025.nc`. Due to the GNET stations not being on a regular grid, each data variable for a time series has been assigned a timestamp and a station identifier. Each station has associated metadata including longitude, latitude, and height.

The NetCDF file contains the following structure:

Coordinates:

- `time`: Timestamp of observations (datetime64)
- `station`: Unique station identifiers (string)

Data Variables:

- `decimalyear` (station, time): Time in decimal year
- `east`, `north`, `up` (station, time): Position components in millimeters
- `east_error`, `north_error`, `up_error` (station, time): Position error estimates in millimeters
- `lat`, `lon` (station): Station coordinates in degrees
- `height` (station): Station height above the reference ellipsoid in meters

6 The Future of GNET and GNSS monitoring in Greenland

GNET forms the basis for the geodetic reference infrastructure in Greenland, and is sponsored directly by the Danish government (The agency of climate data, KDS) through the financial act. For that reason, the network is expected to keep running continuously going forward in time. The network has slowly been expanded over the last few years, with 1 or 2 new GNET stations pr. year. Further expansion of the network depends highly on the funding and the future cost of downloading the raw data. The operational team developing and maintaining GNET plans to establish 2 new GNET sites in the summer of 2026,

https://doi.org/10.5194/essd-2026-198
Preprint. Discussion started: 8 April 2026

at Kap Beaupré (East Greenland) and at Kap Jefferson (Northwest Greenland). As of now, most stations are offline due to the rising cost of the Iridium network. However, with the introduction of satellite to cell connection from commercial entities, it is expected that the near-realtime download of the raw data from all stations can begin again in the near future. The extraction of the data until that point will continue as of now, as part of the maintenance trip in August every year.

7 Conclusion

We present the most extensive processed release of the Greenland GNSS Network (GNET) to date, including observations from pre-GNET cGNSS sites (1995 -) in Greenland together with all GNET stations operating during the period 2007–2025. The dataset comprises position time series from 71 cGNSS stations distributed across the ice-free regions of Greenland.

To assess the quality of the processed time series, two independent evaluation approaches were applied. Noise analysis indicates that the station position time series are consistent with a fractional Gaussian noise behavior, as expected for geodetic-quality GNSS observations. In addition, cross-comparison with previously published subsets of the network produced by JPL and NGL demonstrates improved stability of the horizontal velocity estimates in the new DTU solution.

Alongside the position time series, we provide comprehensive station metadata documenting the evolution of hardware and firmware at each site. The metadata release also includes directional horizon photographs for all GNET antennas, supporting improved interpretation of site-specific environmental influences.

The dataset presented here establishes a consistent and quality-controlled reference for studies within crustal deformation, GIA, and ice-mass change in Greenland. The data product will be regularly updated as additional observations become available and as the GNET network continues to expand.

Appendix A: Velocity Estimates

Derived velocity estimates for the horizontal and vertical components resulting from the GipsyX-2.4 processing. The velocity estimates are found in the individual sumfiles provided here, summarized in Table A1 and visualized in Fig 6. The sumfiles for each station contain the velocity in both the local ENU reference frame and the global Cartesian XYZ coordinates.

Table A1: List of the derived horizontal and vertical linear motion, for each GNET site in the published dataset. The velocity is given as [mm/yr] with an associated estimation error. As listed in Table 1, the newest stations only have sub-3-year time series, which induced an error estimate a magnitude or more larger than older stations.

Station ID	**Location Name**	$\boldsymbol{v}_{East}$ **[mm/yr]**	$\boldsymbol{v}_{North}$ **[mm/yr]**	$\boldsymbol{v}_{Up}$ **[mm/yr]**	$\sigma_{\boldsymbol{v}_{East}}$ **[mm/yr]**	$\sigma_{\boldsymbol{v}_{North}}$ **[mm/yr]**	$\sigma_{\boldsymbol{v}_{Up}}$ **[mm/yr]**
AAS2	Aasiaat	-19.2	11.2	6.3	0.002	0.002	0.007
AASI	Aasiaat	-19.5	11.0	1.6	0.02	0.02	0.07

https://doi.org/10.5194/essd-2026-198
Preprint. Discussion started: 8 April 2026

ASKY	Astrup Kystland	-21.1	9.9	16.0	0.002	0.002	0.008
AVAN	Avannarliit	-18.7	9.6	2.4	0.06	0.08	0.27
BLAS	Blaasø	-12.2	20.5	7.9	0.002	0.002	0.009
DANE	Daneborg	-11.4	20.5	2.3	0.002	0.002	0.009
DGJG	Daugaard-Jensens Glacier	-14.5	18.9	3.5	0.002	0.002	0.008
DKSG	Docker Smith Glacier	-21.4	8.9	13.0	0.001	0.002	0.008
DMHN	Danmarkshavn	-10.6	20.3	3.2	0.002	0.002	0.011
EQNU	Eqaluit Nunataat	-18.8	10.3	1.2	0.06	0.08	0.29
GMMA	Gamma Ø	-10.8	20.1	4.7	0.002	0.002	0.01
GROK	Grønne nunatak	-12.6	19.1	7.4	0.002	0.002	0.009
HEL2	Helheim	-18.3	16.4	16.6	0.001	0.002	0.006
HJOR	Hjørnedal	-15.4	15.9	5.3	0.001	0.002	0.006
HMBG	Hamberg Glacier	-13.9	19.1	0.7	0.002	0.002	0.009
HRDG	Harder Glacier	-18.1	14.0	7.5	0.002	0.002	0.01
ILUL	Ilulissat	-19.2	12.0	7.7	0.001	0.002	0.007
ISOR	Isortoq	-16.6	15.5	7.4	0.002	0.002	0.007
JGBL	Jørgen Brønlund	-14.4	18.2	5.9	0.001	0.002	0.01
JWLF	Jewell Fjord	-18.9	15.1	5.9	0.002	0.002	0.011
KAGA	Kangia	-19.7	12.1	13.5	0.001	0.002	0.006
KAGZ	Kap Agassiz	-22.0	6.2	8.6	0.002	0.002	0.01
KAPI	Kapisilit	-17.8	12.5	2.8	0.002	0.002	0.007
KBUG	Køge Bugt	-17.5	16.1	6.3	0.001	0.002	0.006
KELY	Kellyville	-17.9	11.9	1.7	0.001	0.001	0.004
KLSQ/KLQ3	Kangerlussuaq Black Ridge	-17.8	12.3	2.4	0.003	0.003	0.011
KLY2	Kellyville	-17.2	12.4	-0.0	0.008	0.01	0.033
KMJP	Kap Morris Jessup	-14.8	18.4	4.7	0.002	0.002	0.011
KMOR	Kap Morton	-21.5	7.6	7.5	0.001	0.002	0.009
KSNB	Steenstrup Nordre Glacier	-15.4	18.9	13.7	0.001	0.002	0.006
KSUT	Kitsissut	-17.4	11.2	-2.1	0.03	0.03	0.11
KUAQ	Kangerlussuaq Glacier	-17.1	17.5	17.3	0.002	0.002	0.007
KULL	Kullorsuaq	-21.1	8.9	9.3	0.001	0.002	0.008
KULU	Kulusuk	-15.5	15.6	7.7	0.001	0.001	0.004
LBIB	L. Bistrup Glacier	-12.8	19.1	1.4	0.002	0.002	0.009
LEFN	Leffingwell Nunatak	-13.2	19.2	6.6	0.002	0.002	0.01

https://doi.org/10.5194/essd-2026-198
Preprint. Discussion started: 8 April 2026

LYNS	Lynaes	-15.5	15.9	6.2	0.001	0.002	0.006
MARG	Marie Glacier	-21.9	6.8	7.8	0.001	0.002	0.008
MIK2	Mikisfjord	-15.0	17.5	12.3	0.002	0.002	0.007
MSVG	Mestersvig	-12.0	19.8	3.4	0.002	0.002	0.008
NGFJ	Ingolf fjorden	-10.9	20.4	-2.7	0.07	0.08	0.43
NNVN	North Niviarsiat Nunatak	-17.4	15.5	5.8	0.001	0.002	0.006
NORD	Station Nord	-9.3	21.6	4.0	0.001	0.001	0.008
NRSK	Norske Øer	-9.4	20.9	6.0	0.002	0.002	0.011
NUNA	Nunatarsuaq	-18.7	10.1	1.6	0.06	0.08	0.28
NUUK	Nuuk	-18.1	12.0	1.3	0.001	0.002	0.006
PAMI	Paamiut	-17.5	13.2	0.3	0.004	0.006	0.017
PLPK	Pilappik	-14.6	17.4	10.0	0.002	0.002	0.007
QAQ1	Qaqortoq	-16.6	13.6	3.9	0.001	0.001	0.004
QENU	Qeqetaarsunnguit Nunataat	-18.4	9.4	1.3	0.06	0.08	0.27
QEQE	Qeqertarsuaq	-19.8	11.3	5.8	0.001	0.002	0.006
QAAR	Qaarsut	-19.1	12.1	6.8	0.002	0.002	0.009
RINK	Rink Glacier	-16.8	13.4	7.1	0.001	0.002	0.007
SCBY	Kap Schouby	-20.6	8.7	8.4	0.002	0.002	0.011
SCOB	Ittoqqortoormiit	-10.8	19.2	2.7	0.008	0.012	0.044
SCOR/SCO4	Ittoqqortoormiit	-10.9	20.0	2.2	0.001	0.001	0.005
SENU	Sermip Nunataa	-17.3	13.3	8.1	0.001	0.002	0.006
SISI	Sisimiut	-18.6	11.6	2.8	0.002	0.003	0.009
SRMP	Sermip Nunataa	-21.6	9.8	13.5	0.001	0.002	0.006
THU1	Pituffik Space base	-22.0	5.0	2.3	0.01	0.01	0.061
THU2	Pituffik Space base	-22.5	4.9	6.9	0.001	0.001	0.006
TIMM	Timmiarmiut	-15.2	16.3	6.6	0.001	0.002	0.006
TIN1	Tininilik	-17.8	12.5	4.9	0.004	0.006	0.02
TREO	Trefoldigheden Ø	-16.6	16.1	6.4	0.001	0.002	0.006
UPAK	Uippak	-19.4	14.9	-8.5	0.08	0.11	0.32
UPVK	Upernavik	-21.1	9.8	5.9	0.001	0.002	0.006
UTMG	Timmiarmiit Glacier	-16.9	16.9	6.9	0.002	0.003	0.008
VFDG	Vestfjord Glacier	-14.1	19.5	4.9	0.002	0.002	0.008
WTHG	Walterhausen Glacier	-12.6	19.9	2.4	0.002	0.002	0.008
YMER	Ymer Nunatak	-12.9	19.2	2.7	0.002	0.002	0.009

https://doi.org/10.5194/essd-2026-198
Preprint. Discussion started: 8 April 2026

Open Access Earth System Science Data Discussions

Appendix B: RINEX format data DOI's

Table B1 shows the complete overview of all individual DOI's for RINEX format data from each GNET station. We have chosen to only include the overall DOI's for each station linking to the complete time series. Subset DOI's can be found under each, with the citation request listed specifically at the websites.

Table B1: Overview of DOIs and citations for all individual stations in the network.

Station ID	Location Name	DOI	Citation
AAS2	Aasiaat	https://doi.org/10.60888/EPOS-GNSS-AAS200GRL	KDS (2026d)
AASI	Aasiaat	https://doi.org/10.60888/EPOS-GNSS-AASI00GRL	KDS (2026e)
ASKY	Astrup Kystland	https://doi.org/10.7283/W70R-JA23	KDS et al. (2007a)
AVAN	Avannarliit	https://doi.org/10.60888/EPOS-GNSS-AVAN00GRL	KDS (2026f)
BLAS	Blaasø	https://doi.org/10.7283/SCBP-5753	KDS et al. (2008a)
DANE	Daneborg	https://doi.org/10.7283/J5AS-ZN66	KDS et al. (2009a)
DGJG	Daugaard-Jensens Glacier	https://doi.org/10.7283/S3EH-XJ14	KDS et al. (2009b)
DKSG	Docker Smith Glacier	https://doi.org/10.7283/C4AR-3924	KDS et al. (2007b)
DMHN	Danmarkshavn	https://doi.org/10.60888/EPOS-GNSS-DMHN00GRL	KDS (2026g)
EQNU	Eqaluit Nunataat	https://doi.org/10.60888/EPOS-GNSS-EQNU00GRL	KDS (2026h)
GMMA	Gamma Ø	https://doi.org/10.7283/B78A-BZ29	KDS et al. (2009c)
GROK	Grønne nunatak	https://doi.org/10.7283/SPX7-V408	KDS et al. (2008b)
HEL2	Helheim Glacier	https://doi.org/10.7283/7PB0-2Z53	KDS et al. (2007c)
HJOR	Hjørnedal	https://doi.org/10.7283/J6TF-HA29	KDS et al. (2007d)
HMBG	Hamburg Glacier	https://doi.org/10.7283/6224-KD23	KDS et al. (2009d)
HRDG	Harder Glacier	https://doi.org/10.7283/FXP4-4M53	KDS et al. (2008c)
ILUL	Ilulissat	https://doi.org/10.60888/EPOS-GNSS-ILUL00GRL	KDS (2026i)
ISOR	Isortoq	https://doi.org/10.60888/EPOS-GNSS-ISOR00GRL	KDS (2026j)
JGBL	Jørgen Brønlund	https://doi.org/10.7283/RDME-K197	KDS et al. (2008d)
JWLF	Jewell Fjord	https://doi.org/10.7283/XTG2-A936	KDS et al. (2008e)
KAGA	Kangia	https://doi.org/10.7283/FQGY-4535	KDS et al. (2006)
KAGZ	Kap Agassiz	https://doi.org/10.7283/B6AB-0X85	KDS et al. (2007e)
KAPI	Kapisilit	https://doi.org/10.60888/EPOS-GNSS-KAPI00GRL	KDS (2026k)
KBUG	Køge Bugt	https://doi.org/10.7283/KYQM-YH78	KDS et al. (2007f)

https://doi.org/10.5194/essd-2026-198
Preprint. Discussion started: 8 April 2026

KELY	Kellyville	https://doi.org/10.24414/ROB-EUREF-KELY00GRL	KDS (2026l)
KLSQ	Kangerlussuaq Black Ridge	https://doi.org/10.24414/ROB-EUREF-KLSQ00GRL	DTU Space (2025a)
KLQ3	Kangerlussuaq Black Ridge	https://doi.org/10.60888/EPOS-GNSS-KLQ300GRL	KDS (2026m)
KLY2	Kellyville	https://doi.org/10.60888/EPOS-GNSS-KLY200GRL	KDS (2026n)
KMJP	Kap Morris Jessup	https://doi.org/10.7283/37CW-0G31	KDS et al. (2008f)
KMOR	Kap Morton	https://doi.org/10.7283/5A7T-P404	KDS et al. (2007g)
KSNB	Steenstrup Nordre Glacier	https://doi.org/10.7283/RHVV-9P67	KDS et al. (2007h)
KSUT	Kitsissut	https://doi.org/10.60888/EPOS-GNSS-KSUT00GRL	KDS (2026o)
KUAQ	Kangerlussuaq Glacier	https://doi.org/10.7283/HQ0D-3D69	KDS et al. (2009e)
KULL	Kullorsuaq	https://doi.org/10.60888/EPOS-GNSS-KULL00GRL	KDS (2026a)
KULU	Kulusuk	https://doi.org/10.60888/EPOS-GNSS-KULU00GRL	KDS (2026b)
LBIB	L. Bistrup Glacier	https://doi.org/10.7283/JJJP-BC78	KDS et al. (2009f)
LEFN	Leffingwell Nunatak	https://doi.org/10.7283/NW2Q-7G38	KDS et al. (2008g)
LYNS	Lynaes	https://doi.org/10.7283/B41P-6468	KDS et al. (2007i)
MARG	Marie Glacier	https://doi.org/10.7283/432P-NT47	KDS et al. (2007j)
MIK2	Mikisfjord	https://doi.org/10.7283/ABT9-NF76	KDS et al. (2009g)
MSVG	Mestersvig	https://doi.org/10.7283/SMV9-Y888	KDS et al. (2009h)
NGFJ	Ingolf fjorden	https://doi.org/10.60888/EPOS-GNSS-NGFJ00GRL	KDS (2026p)
NNVN	North Niviarsiat Nunatak	https://doi.org/10.7283/T5PH-B743	KDS et al. (2007k)
NORD	Station Nord	https://doi.org/10.60888/EPOS-GNSS-NORD00GRL	KDS (2026q)
NRSK	Norske Øer	https://doi.org/10.7283/T7MX-RH72	KDS et al. (2008h)
NUNA	Nunatarsuaq	https://doi.org/10.60888/EPOS-GNSS-NUNA00GRL	KDS (2026r)
NUUK	Nuuk	https://doi.org/10.60888/EPOS-GNSS-NUUK00GRL	KDS (2026s)
PAMI	Paamiut	https://doi.org/10.60888/EPOS-GNSS-PAMI00GRL	KDS (2026t)
PLPK	Pilappik	https://doi.org/10.7283/QQJP-4H93	KDS et al. (2007l)
QAQ1	Qaqortoq	https://doi.org/10.24414/ROB-EUREF-QAQ100GRL	DTU Space (2025b)
QENU	Qeqetaarsunnguit Nunataat	https://doi.org/10.60888/EPOS-GNSS-QENU00GRL	KDS (2026u)

https://doi.org/10.5194/essd-2026-198
Preprint. Discussion started: 8 April 2026

QEQE	Qeqertarsuaq	https://doi.org/10.60888/EPOS-GNSS-QEQE00GRL	KDS (2026v)
QAAR	Qaarsut	https://doi.org/10.60888/EPOS-GNSS-QAAR00GRL	KDS (2026c)
RINK	Rink Glacier	https://doi.org/10.7283/NAQ5-7H44	KDS et al. (2007m)
SCBY	Kap Schouby	https://doi.org/10.7283/EWF4-Z744	KDS et al. (2007n)
SCOB	Ittoqqortoormiit	https://doi.org/10.11583/DTU.31678426	Solgaard et al. (2026ab)
SCO4	Ittoqqortoormiit	https://doi.org/10.60888/EPOS-GNSS-SCO400GRL	KDS (2026w)
SCOR	Ittoqqortoormiit	https://doi.org/10.24414/ROB-EUREF-SCOR00GRL	DTU Space (2025c)
SENU	Sermip Nunataa	https://doi.org/10.7283/NVG7-3K93	KDS et al. (2008i)
SISI	Sisimiut	https://doi.org/10.60888/EPOS-GNSS-SISI00GRL	KDS (2026x)
SRMP	Sermip Nunataa	https://doi.org/10.7283/PJRV-T540	KDS et al. (2007o)
THU1	Pituffik Space base	https://doi.org/10.11583/DTU.31673032	Solgaard et al. (2026ac)
THU2	Pituffik Space base	https://doi.org/10.24414/ROB-EUREF-THU200GRL	DTU Space (2025d)
TIMM	Timmiarmiut	https://doi.org/10.7283/C4AR-3924	KDS et al. (2007p)
TIN1	Tininilik	https://doi.org/10.60888/EPOS-GNSS-TIN100GRL	KDS (2026y)
TREO	Trefoldigheden Ø	https://doi.org/10.7283/QDN6-X096	KDS et al. (2007q)
UPAK	Uippak	https://doi.org/10.60888/EPOS-GNSS-UPAK00GRL	KDS (2026z)
UPVK	Upernavik	https://doi.org/10.60888/EPOS-GNSS-UPVK00GRL	KDS (2026aa)
UTMG	Timmiarmiit Glacier	https://doi.org/10.7283/0ZZ3-VV92	KDS et al. (2007r)
VFDG	Vestfjord Glacier	https://doi.org/10.7283/VT9V-WH52	KDS et al. (2009i)
WTHG	Walterhausen Glacier	https://doi.org/10.7283/12FV-AQ34	KDS et al. (2009j)
YMER	Ymer Nunatak	https://doi.org/10.7283/2GBV-B806	KDS et al. (2009k)

Author contributions. CS conceptualized the study with inputs from SAK and DLB. FBM, THN, OB, SAK, MWD, and CS were involved in the collection of the observational data and the station metadata. SAK processed the position time series for all sites with DLB, compiling the processed NetCDF file. CS conducted the dataset validation process. CS wrote the majority of the paper, with SAB writing the processing section and FBM writing the historic GNSS station part. CS compiled most of the figures included, with DLB contributing one figure.

Competing interests. The authors declare that they have no conflict of interest.

https://doi.org/10.5194/essd-2026-198
Preprint. Discussion started: 8 April 2026

Acknowledgements. S. A. Khan acknowledges support from the Novo Nordisk Foundation under the Challenge Programme 2023—Grant NNF23OC00807040. We thank the Danish Agency for Climate Data for providing the GNET GNSS data. Lastly we want to acknowledge all former contributors and operators that have worked with the network, we extend our gratitude to: Eric Kendric, Dana Caccamise, Michael Wilis, Jian Wang (Ohio State University, USA), Bjorn Johns, Seth White, Jeremy Miner (UNAVCO, USA), Arne V. Olesen, and Emil Nielsen (DTU SPACE, Denmark).

https://doi.org/10.5194/essd-2026-198
Preprint. Discussion started: 8 April 2026

References

Altamimi, Z., Rebischung, P., Collilieux, X., Métivier, L., and Chanard, K.: ITRF2020: an augmented reference frame refining the modeling of nonlinear station motions, Journal of Geodesy, 97, 47, https://doi.org/10.1007/s00190-023-01738-w, 2023.

Aster, R. C., Borchers, B., and Thurber, C.: Parameter Estimation and Inverse Problems, Tech. rep., 2004.

Barletta, V. R., Bordoni, A., and Khan, S. A.: GNET Derived Mass Balance and Glacial Isostatic Adjustment Constraints for Greenland, Geophysical Research Letters, 51, https://doi.org/10.1029/2023GL106891, 2024.

Berg, D., Barletta, V. R., Hassan, J., Lippert, E. Y., Colgan, W., Bevis, M., Steffen, R., and Khan, S. A.: Vertical Land Motion Due To Present-Day Ice Loss From Greenland's and Canada's Peripheral Glaciers, Geophysical Research Letters, 51, https://doi.org/10.1029/2023GL104851, 2024.

Berg, D. L., Adhikari, S., Hassan, J., Steffen, R., Steffen, H., Willis, M., and Khan, S. A.: Estimation and Attribution of Horizontal Land Motion Measured by the Greenland GNSS Network, Journal of Geophysical Research: Solid Earth, 130, https://doi.org/10.1029/2024JB030847, 2025.

Bertiger, W., Bar-Sever, Y., Dorsey, A., Haines, B., Harvey, N., Hemberger, D., Heflin, M., Lu, W., Miller, M., Moore, A. W., Murphy, D., Ries, P., Romans, L., Sibois, A., Sibthorpe, A., Szilagyi, B., Vallisneri, M., and Willis, P.: GipsyX/RTGx, a new tool set for space geodetic operations and research, Advances in Space Research, 66, 469–489, https://doi.org/10.1016/j.asr.2020.04.015, 2020.

Bevis, M. and Brown, A.: Trajectory models and reference frames for crustal motion geodesy, Journal of Geodesy, 88, 283–311, https://doi.org/10.1007/s00190-013-0685-5, 2014.

Bevis, M., Wahr, J., Khan, S. A., Bo Madsen, F., Brown, A., Willis, M., Kendrick, E., Knudsen, P., Box, J. E., van Dam, T., Caccamise II, D. J., Johns, B., Nylen, T., Abbott, R., White, S., Miner, J., Forsberg, R., Zhou, H., Wang, J., Wilson, T., Bromwich, D., and Francis, O.: Bedrock displacements in Greenland manifest ice mass variations, climate cycles and climate change, https://doi.org/10.1073/pnas.1204664109/-/DCSupplemental, 2012.

Bevis, M., Harig, C., Khan, S. A., Brown, A., Simons, F. J., Willis, M., Fettweis, X., Van Den Broeke, M. R., Madsen, F. B., Kendrick, E., Caccamise, D. J., Van Dam, T., Knudsen, P., and Nylen, T.: Accelerating changes in ice mass within Greenland, and the ice sheet's sensitivity to atmospheric forcing, Proceedings of the National Academy of Sciences of the United States of America, 116, 1934–1939, https://doi.org/10.1073/pnas.1806562116, 2019.

Bian, Y., Li, Z., Huang, Z., He, B., Shi, L., and Miao, S.: Combined GRACE and GPS to Analyze the Seasonal Variation of Surface Vertical Deformation in Greenland and Its Influence, Remote Sensing, 15, https://doi.org/10.3390/rs15020511, 2023.

Blewitt, G., Hammond, W. C., and Kreemer, C.: Harnessing the GPS Data Explosion for Interdisciplinary Science, Eos, 99, https://doi.org/10.1029/2018EO104623, 2018.

Boehm, J., Niell, A., Tregoning, P., and Schuh, H.: Global Mapping Function (GMF): A new empirical mapping function based on numerical weather model data, Geophysical Research Letters, 33, https://doi.org/10.1029/2005GL025546, 2006.

Buchta, E., Scheinert, M., King, M. A., Wilson, T., Koulali, A., Clarke, P. J., Gómez, D., Kendrick, E., Knöfel, C., and Busch, P.: Advancing geodynamic research in Antarctica: reprocessing GNSS data to infer consistent coordinate time series (GIANT-REGAIN), Earth System Science Data, 17, 1761–1780, https://doi.org/10.5194/essd-17-1761-2025, 2025.

Carrére, L., Lyard, F., Cancet, M., Guillot, A., and Picot, N.: FES 2014, a new tidal model—validation results and perspectives for improvements, in: Proceedings of the ESA Living Planet Symposium, pp. 9–13, Prague, Czech Republic, 2016.

Danish Agency for Climate Data (KDS): GNSS – Grønland [Dataset], https://dataforsyningen.dk/data/4804, 2026.

https://doi.org/10.5194/essd-2026-198
Preprint. Discussion started: 8 April 2026

DTU Space: GNSS data of KLSQ00GRL, Kangerlussuaq, Greenland, https://doi.org/10.24414/ROB-EUREF-KLSQ00GRL, 2025a.

DTU Space: GNSS data of QAQ100GRL, Qaqortoq / Julianehaab, Greenland, https://doi.org/10.24414/ROB-EUREF-QAQ100GRL, 2025b.

DTU Space: GNSS data of SCOR00GRL, Scoresbysund/Ittoqqoormiit, Greenland, https://doi.org/10.24414/ROB-EUREF-SCOR00GRL, 2025c.

DTU Space: GNSS data of THU200GRL, Thule Airbase, Greenland, https://doi.org/10.24414/ROB-EUREF-THU200GRL, 2025d.

Fisher, M., Stafford, T., Moon, T., and Thurber, A.: QGreenland, https://doi.org/10.5281/zenodo.8326507, 2023.

Goudarzi, M. A., Cocard, M., and Santerre, R.: Noise behavior in CGPS position time series: The Eastern North America case study, Journal of Geodetic Science, 5, 119–147, https://doi.org/10.1515/jogs-2015-0013, 2015.

Greene, C. A., Gardner, A. S., Wood, M., and Cuzzone, J. K.: Ubiquitous acceleration in Greenland Ice Sheet calving from 1985 to 2022, Nature, 625, 523–528, https://doi.org/10.1038/s41586-023-06863-2, 2024.

Hawley, R. and Brunt, K.: The Future Shape of the Greenland Geodetic Network (GNET), https://www.arcus.org/witness-the-arctic/2019/12/highlight/1, 2019.

Hawley, R., Ivins, E., Neumann, T., Adhikari, S., Andrews, L., Babonis, G., Bevis, M., Bromwich, D., Chew, C., Christensen, S., Crain, R., Csatho, B., Forsberg, R., Grapenthin, R., Khan, S. A., Kjeldsen, K. K., Knudsen, P., Larour, E., Bo Madsen, F., Mattiolli, G., Nylen, T., Dev Singh, K., van Dam, T., and Willis, M.: GNET 2017 Forward: The Future Shape of a Greenland GNSS Observation Network, Tech. rep., NASA Goddard Space Flight Center / National Science Foundation Workshop, https://go-gnet.org/Media/638059156160053022/GNETwhitepaper.pdf, 2017.

Heflin, M., Donnellan, A., Parker, J., Lyzenga, G., Moore, A., Ludwig, L. G., Rundle, J., Wang, J., and Pierce, M.: Automated Estimation and Tools to Extract Positions, Velocities, Breaks, and Seasonal Terms From Daily GNSS Measurements: Illuminating Nonlinear Salton Trough Deformation, Earth and Space Science, 7, https://doi.org/10.1029/2019EA000644, 2020.

International GNSS Service: IGS Network, https://network.igs.org/, 2026.

International GNSS Service (IGS): Guidelines for Continuously Operating Reference Stations in the IGS, https://files.igs.org/pub/resource/guidelines/Guidelines_for_Continuously_Operating_Reference_Stations_in_the_IGS_v1.0.pdf, 2023.

KDS: GNSS data of KULL00GRL, Kullorsuaq, Greenland, https://doi.org/10.60888/EPOS-GNSS-KULL00GRL, 2026a.

KDS: GNSS data of KULU00GRL, Kulusuk, Greenland, https://doi.org/10.60888/EPOS-GNSS-KULU00GRL, 2026b.

KDS: GNSS data of QAAR00GRL, Quaarsuut, Greenland, https://doi.org/10.60888/EPOS-GNSS-QAAR00GRL, 2026c.

KDS: GNSS data of AAS200GRL, Aasiaat, Greenland, https://doi.org/10.60888/EPOS-GNSS-AAS200GRL, 2026d.

KDS: GNSS data of AASI00GRL, Aasiaat, Greenland, https://doi.org/10.60888/EPOS-GNSS-AASI00GRL, 2026e.

KDS: GNSS data of AVAN00GRL, Avannarliit, Greenland, https://doi.org/10.60888/EPOS-GNSS-AVAN00GRL, 2026f.

KDS: GNSS data of DMHN00GRL, Danmarkshavn, Greenland, https://doi.org/10.60888/EPOS-GNSS-DMHN00GRL, 2026g.

KDS: GNSS data of EQNU00GRL, Eqaluit Nunataat, Greenland, https://doi.org/10.60888/EPOS-GNSS-EQNU00GRL, 2026h.

KDS: GNSS data of ILUL00GRL, Ilulissat, Greenland, https://doi.org/10.60888/EPOS-GNSS-ILUL00GRL, 2026i.

KDS: GNSS data of ISOR00GRL, Isortoq, Greenland, https://doi.org/10.60888/EPOS-GNSS-ISOR00GRL, 2026j.

KDS: GNSS data of KAPI00GRL, Kapisillit, Greenland, https://doi.org/10.60888/EPOS-GNSS-KAPI00GRL, 2026k.

KDS: GNSS data of KELY00GRL, Kangerlussuaq, Greenland, https://doi.org/10.24414/ROB-EUREF-KELY00GRL, 2026l.

KDS: GNSS data of KLQ300GRL, Kangerlussuaq, Greenland, https://doi.org/10.60888/EPOS-GNSS-KLQ300GRL, 2026m.

KDS: GNSS data of KLY200GRL, Kellyville 2, Greenland, https://doi.org/10.60888/EPOS-GNSS-KLY200GRL, 2026n.

KDS: GNSS data of KSUT00GRL, Nuuk, Greenland, https://doi.org/10.60888/EPOS-GNSS-KSUT00GRL, 2026o.

https://doi.org/10.5194/essd-2026-198
Preprint. Discussion started: 8 April 2026

KDS: GNSS data of NGFJ00GRL, Ingolf Fjord, Greenland, https://doi.org/10.60888/EPOS-GNSS-NGFJ00GRL, 2026p.

KDS: GNSS data of NORD00GRL, Station Nord, Greenland, https://doi.org/10.60888/EPOS-GNSS-NORD00GRL, 2026q.

KDS: GNSS data of NUNA00GRL, Nunatarsuaq, Greenland, https://doi.org/10.60888/EPOS-GNSS-NUNA00GRL, 2026r.

KDS: GNSS data of NUUK00GRL, Nuuk, Greenland, https://doi.org/10.60888/EPOS-GNSS-NUUK00GRL, 2026s.

KDS: GNSS data of PAMI00GRL, Paamiut, Greenland, https://doi.org/10.60888/EPOS-GNSS-PAMI00GRL, 2026t.

KDS: GNSS data of QENU00GRL, Qeqetaarsunnguit Nunataat, Greenland, https://doi.org/10.60888/EPOS-GNSS-QENU00GRL, 2026u.

KDS: GNSS data of QEQE00GRL, Qeqertarsuaq (Godhavn), Greenland, https://doi.org/10.60888/EPOS-GNSS-QEQE00GRL, 2026v.

KDS: GNSS data of SCO400GRL, Scoresbysund/Ittoqqoormiit, Greenland, https://doi.org/10.60888/EPOS-GNSS-SCO400GRL, 2026w.

KDS: GNSS data of SISI00GRL, Sisimiut, Greenland, https://doi.org/10.60888/EPOS-GNSS-SISI00GRL, 2026x.

KDS: GNSS data of TIN100GRL, Tininnilik, Greenland, https://doi.org/10.60888/EPOS-GNSS-TIN100GRL, 2026y.

KDS: GNSS data of UPAK00GRL, Uippak, Greenland, https://doi.org/10.60888/EPOS-GNSS-UPAK00GRL, 2026z.

KDS: GNSS data of UPVK00GRL, Upernavik, Greenland, https://doi.org/10.60888/EPOS-GNSS-UPVK00GRL, 2026aa.

KDS, Community, U., Fahnestock, M., and Truffer, M.: Greenland GNSS Network - KAGA-Kangia North P.S. - GPS/GNSS Observations Dataset, https://doi.org/10.7283/FQGY-4535, 2006.

KDS, Community, U., and Bevis, M.: Greenland GNSS Network - ASKY-Astrup Kystland P.S. - GPS/GNSS Observations Dataset, https://doi.org/10.7283/W70R-JA23, 2007a.

KDS, Community, U., and Bevis, M.: Greenland GNSS Network - DKSG-Doecker Smith Gletscher P.S. - GPS/GNSS Observations Dataset, https://doi.org/10.7283/C4AR-3924, 2007b.

KDS, Community, U., and Bevis, M.: Greenland GNSS Network - HEL2-Helheim Glacier P.S. - GPS/GNSS Observations Dataset, https://doi.org/10.7283/7PB0-2Z53, 2007c.

KDS, Community, U., and Bevis, M.: Greenland GNSS Network - HJOR-Hjornefjeldet P.S. - GPS/GNSS Observations Dataset, https://doi.org/10.7283/J6TF-HA29, 2007d.

KDS, Community, U., and Bevis, M.: Greenland GNSS Network - KAGZ-Kap Agassiz P.S. - GPS/GNSS Observations Dataset, https://doi.org/10.7283/B6AB-0X85, 2007e.

KDS, Community, U., and Bevis, M.: Greenland GNSS Network - KBUG-Koge Bugt P.S. - GPS/GNSS Observations Dataset, https://doi.org/10.7283/KYQM-YH78, 2007f.

KDS, Community, U., and Bevis, M.: Greenland GNSS Network - KMOR-Kap Morton P.S. - GPS/GNSS Observations Dataset, https://doi.org/10.7283/5A7T-P404, 2007g.

KDS, Community, U., and Bevis, M.: Greenland GNSS Network - KSNB-Steenstrup Nordre Brae P.S. - GPS/GNSS Observations Dataset, https://doi.org/10.7283/RHVV-9P67, 2007h.

KDS, Community, U., and Bevis, M.: Greenland GNSS Network - LYNS-Lynaes P.S. - GPS/GNSS Observations Dataset, https://doi.org/10.7283/B41P-6468, 2007i.

KDS, Community, U., and Bevis, M.: Greenland GNSS Network - MARG-Marie Gletscher P.S. - GPS/GNSS Observations Dataset, https://doi.org/10.7283/432P-NT47, 2007j.

KDS, Community, U., and Bevis, M.: Greenland GNSS Network - NNVN-North Niviarsiat Nunatak P.S. - GPS/GNSS Observations Dataset, https://doi.org/10.7283/T5PH-B743, 2007k.

KDS, Community, U., and Bevis, M.: Greenland GNSS Network - PLPK-Pilappik P.S. - GPS/GNSS Observations Dataset, https://doi.org/10.7283/QQJP-4H93, 2007l.

https://doi.org/10.5194/essd-2026-198
Preprint. Discussion started: 8 April 2026

KDS, Community, U., and Bevis, M.: Greenland GNSS Network - RINK-Rinks Isbrae P.S. - GPS/GNSS Observations Dataset, https://doi.org/10.7283/NAQ5-7H44, 2007m.

KDS, Community, U., and Bevis, M.: Greenland GNSS Network - SCBY-Kap Schoubye P.S. - GPS/GNSS Observations Dataset, https://doi.org/10.7283/EWF4-Z744, 2007n.

KDS, Community, U., and Bevis, M.: Greenland GNSS Network - SRMP-Sermip Nuunataa P.S. - GPS/GNSS Observations Dataset, https://doi.org/10.7283/PJRV-T540, 2007o.

KDS, Community, U., and Bevis, M.: Greenland GNSS Network - TIMM-Timmiarmiut P.S. - GPS/GNSS Observations Dataset, https://doi.org/10.7283/QDN6-X096, 2007p.

KDS, Community, U., and Bevis, M.: Greenland GNSS Network - TREO-Trefoldighedens O P.S. - GPS/GNSS Observations Dataset, https://doi.org/10.7283/VH5H-PX24, 2007q.

KDS, Community, U., and Bevis, M.: Greenland GNSS Network - UTMG-Upper Timmiarmiit Glacier P.S. - GPS/GNSS Observations Dataset, https://doi.org/10.7283/0ZZ3-VV92, 2007r.

KDS, Community, U., and Bevis, M.: Greenland GNSS Network - BLAS-Blaasor P.S. - GPS/GNSS Observations Dataset, https://doi.org/10.7283/SCBP-5753, 2008a.

KDS, Community, U., and Bevis, M.: Greenland GNSS Network - GROK-Gronne Nunatak P.S. - GPS/GNSS Observations Dataset, https://doi.org/10.7283/SPX7-V408, 2008b.

KDS, Community, U., and Bevis, M.: Greenland GNSS Network - HRDG-Harder Gletscher P.S. - GPS/GNSS Observations Dataset, https://doi.org/10.7283/FXP4-4M53, 2008c.

KDS, Community, U., and Bevis, M.: Greenland GNSS Network - JGBL-Jorgen Bronlund P.S. - GPS/GNSS Observations Dataset, https://doi.org/10.7283/RDME-K197, 2008d.

KDS, Community, U., and Bevis, M.: Greenland GNSS Network - JWLF-Jewell Fjord P.S. - GPS/GNSS Observations Dataset, https://doi.org/10.7283/XTG2-A936, 2008e.

KDS, Community, U., and Bevis, M.: Greenland GNSS Network - KMJP-Kap Morris Jessup P.S. - GPS/GNSS Observations Dataset, https://doi.org/10.7283/37CW-0G31, 2008f.

KDS, Community, U., and Bevis, M.: Greenland GNSS Network - LEFN-Leffingwell Nunatak P.S. - GPS/GNSS Observations Dataset, https://doi.org/10.7283/NW2Q-7G38, 2008g.

KDS, Community, U., and Bevis, M.: Greenland GNSS Network - NRSK-Norske Oye P.S. - GPS/GNSS Observations Dataset, https://doi.org/10.7283/T7MX-RH72, 2008h.

KDS, Community, U., and Bevis, M.: Greenland GNSS Network - SENU-Sermip Nunataa P.S. - GPS/GNSS Observations Dataset, https://doi.org/10.7283/NVG7-3K93, 2008i.

KDS, Community, U., and Bevis, M.: Greenland GNSS Network - DANE-Daneborg P.S. - GPS/GNSS Observations Dataset, https://doi.org/10.7283/J5AS-ZN66, 2009a.

KDS, Community, U., and Bevis, M.: Greenland GNSS Network - DGJG-Daugaard Jensen Gletshcer P.S. - GPS/GNSS Observations Dataset, https://doi.org/10.7283/S3EH-XJ14, 2009b.

KDS, Community, U., and Bevis, M.: Greenland GNSS Network - GMMA-Gamma O P.S. - GPS/GNSS Observations Dataset, https://doi.org/10.7283/B78A-BZ29, 2009c.

KDS, Community, U., and Bevis, M.: Greenland GNSS Network - HMBG-Hamburg Gletshcer P.S. - GPS/GNSS Observations Dataset, https://doi.org/10.7283/6224-KD23, 2009d.

https://doi.org/10.5194/essd-2026-198
Preprint. Discussion started: 8 April 2026

KDS, Community, U., and Bevis, M.: Greenland GNSS Network - KUAQ-Kangerdlussuaq Gletshcer P.S. - GPS/GNSS Observations Dataset, https://doi.org/10.7283/HQ0D-3D69, 2009e.

KDS, Community, U., and Bevis, M.: Greenland GNSS Network - LBIB-L. Bistrup Is Brae P.S. - GPS/GNSS Observations Dataset, https://doi.org/10.7283/JJJP-BC78, 2009f.

KDS, Community, U., and Bevis, M.: Greenland GNSS Network - MIK2-Mikis Fjord P.S. - GPS/GNSS Observations Dataset, https://doi.org/10.7283/ABT9-NF76, 2009g.

KDS, Community, U., and Bevis, M.: Greenland GNSS Network - MSVG-Mestersvig P.S. - GPS/GNSS Observations Dataset, https://doi.org/10.7283/SMV9-Y888, 2009h.

KDS, Community, U., and Bevis, M.: Greenland GNSS Network - VFDG-Vestfjord Gletscher P.S. - GPS/GNSS Observations Dataset, https://doi.org/10.7283/VT9V-WH52, 2009i.

KDS, Community, U., and Bevis, M.: Greenland GNSS Network - WTHG-Walterhausen Gletshcer P.S. - GPS/GNSS Observations Dataset, https://doi.org/10.7283/12FV-AQ34, 2009j.

KDS, Community, U., and Bevis, M.: Greenland GNSS Network - YMER-Ymer Nunatak P.S. - GPS/GNSS Observations Dataset, https://doi.org/10.7283/2GBV-B806, 2009k.

Khan, S. A., Liu, L., Wahr, J., Howat, I., Joughin, I., Van Dam, T., and Fleming, K.: GPS measurements of crustal uplift near Jakobshavn Isbræ due to glacial ice mass loss, Journal of Geophysical Research: Solid Earth, 115, https://doi.org/10.1029/2010JB007490, 2010.

Khan, S. A., Wahr, J., Bevis, M., Velicogna, I., and Kendrick, E.: Spread of ice mass loss into northwest Greenland observed by GRACE and GPS, Geophysical Research Letters, 37, https://doi.org/10.1029/2010GL042460, 2010ab.

Khan, S. A., Sasgen, I., Bevis, M., Van Dam, T., Bamber, J. L., Willis, M., Kjær, K. H., Wouters, B., Helm, V., Csatho, B., Fleming, K., Bjørk, A. A., Aschwanden, A., Knudsen, P., and Munneke, P. K.: Geodetic measurements reveal similarities between post–Last Glacial Maximum and present-day mass loss from the Greenland ice sheet, Science Advances, 2, https://doi.org/10.1126/sciadv.1600931, 2016.

Kjeldsen, K. K., Khan, S. A., Wahr, J., Korsgaard, N. J., Kjær, K. H., Bjørk, A. A., Hurkmans, R., Van Den Broeke, M. R., Bamber, J. L., and Van Angelen, J. H.: Improved ice loss estimate of the northwestern Greenland ice sheet, Journal of Geophysical Research: Solid Earth, 118, 698–708, https://doi.org/10.1029/2012JB009684, 2013.

Larson, K. M., Ray, R. D., Nievinski, F. G., and Freymueller, J. T.: The accidental tide gauge: A GPS reflection case study from kachemak bay, Alaska, IEEE Geoscience and Remote Sensing Letters, 10, 1200–1204, https://doi.org/10.1109/LGRS.2012.2236075, 2013.

Liu, L., Khan, S. A., van Dam, T., Ma, J. H. Y., and Bevis, M.: Annual variations in GPS-measured vertical displacements near Upernavik Isstrøm (Greenland) and contributions from surface mass loading, Journal of Geophysical Research: Solid Earth, 122, 677–691, https://doi.org/10.1002/2016JB013494, 2017.

Materna, K., Feng, L., Lindsey, E. O., Hill, E. M., Ahsan, A., Alam, A. K., Oo, K. M., Than, O., Aung, T., Khaing, S. N., and Bürgmann, R.: GNSS characterization of hydrological loading in South and Southeast Asia, Geophysical Journal International, 224, 1742–1752, https://doi.org/10.1093/gji/ggaa500, 2021.

Montillet, J.-P. and Bos Editors, M. S.: Springer Geophysics Geodetic Time Series Analysis in Earth Sciences, Tech. rep., Springer Geophysics, ISBN 978-3-030-21717-4, ISSN 2364-9119, http://www.springer.com/series/10173, 2020.

NASA Jet Propulsion Laboratory: JPL GPS Time Series (repro2018a), https://sideshow.jpl.nasa.gov/pub/JPL_GPS_Timeseries/repro2018a/post/point/, 2018.

https://doi.org/10.5194/essd-2026-198
Preprint. Discussion started: 8 April 2026

Nielsen, K., Khan, S. A., Korsgaard, N. J., Kjær, K. H., Wahr, J., Bevis, M., Stearns, L. A., and Timm, L. H.: Crustal uplift due to ice mass variability on Upernavik Isstrøm, west Greenland, Earth and Planetary Science Letters, 353-354, 182–189, https://doi.org/10.1016/j.epsl.2012.08.024, 2012.

Seeber, G.: Seeber · Satellite Geodesy, de Gruyter, 2nd edition edn., ISBN 3-11-017569-5, 2003.

Septentrio: PolaRx5: Multi-frequency, multi-constellation GNSS Reference Receiver, https://www.septentrio.com/en/products/gnss-receivers/gnss-reference-receivers/polarx-5, 2025.

Simpson, M. J., Wake, L., Milne, G. A., and Huybrechts, P.: The influence of decadal- to millennial-scale ice mass changes on present-day vertical land motion in Greenland: Implications for the interpretation of GPS observations, Journal of Geophysical Research: Solid Earth, 116, https://doi.org/10.1029/2010JB007776, 2011.

Solgaard, C., Nordmann Winther-Dahl, M., Nylen, T., Madsen, F. B., Hansen, O. B., Berg, D. L., Hassan, J., Knudsen, P., Bevis, M., and Khan, S. A.: Daily coordinate time series from the Greenland GNSS Network (GNET) from 1995–2025 [Dataset], https://doi.org/10.11583/DTU.31397901, 2026.

Solgaard, C., Nordmann Winther-Dahl, M., Nylen, T., Madsen, F. B., Hansen, O. B., Berg, D. L., Hassan, J., Knudsen, P., Bevis, M., and Khan, S. A.: SCOB daily RINEX2 30s files from 1997 - 2005 [Dataset], https://doi.org/10.11583/DTU.31678426, 2026ab.

Solgaard, C., Nordmann Winther-Dahl, M., Nylen, T., Madsen, F. B., Hansen, O. B., Berg, D. L., Hassan, J., Knudsen, P., Bevis, M., and Khan, S. A.: THU1 daily RINEX2 30s files from 1995 - 2003 [Dataset], https://doi.org/10.11583/DTU.31673032, 2026ac.

The Danish Agency for Climate Data (Klimadatastyrelsen): GNET – Greenland GNSS Network, https://www.eng.klimadatastyrelsen.dk/green-transition-and-climate-adaptation/gnet, https://www.eng.klimadatastyrelsen.dk/green-transition-and-climate-adaptation/gnet, 2026.

UNAVCO Inc.: NSF GAGE — Measuring Our Changing Earth, https://www.unavco.org/, https://www.unavco.org/, 2026.

White, A. M., Gardner, W. P., Borsa, A. A., Argus, D. F., and Martens, H. R.: A Review of GNSS/GPS in Hydrogeodesy: Hydrologic Loading Applications and Their Implications for Water Resource Research, https://doi.org/10.1029/2022WR032078, 2022.

Xeos Technologies Inc.: Resolute: All-in-one GNSS monitoring receiver, https://xeostech.com/resolute, 2024.